Highlights

- The concentration of fluoride doesn’t reflect the rate of fluoride release.
- Calcium phosphate formula and/or additives would influence fluoride ion release.
- CPP-ACP or Bioglass® could be source of bioavailable calcium and phosphate.

Abstract

Objective. To compare ion release characteristics of three different dental varnishes either containing CPP-ACP and fluoride (CPP-ACPF, MI Varnish GC, Japan), bioactive glass and fluoride (BGAF, Dentsply Sirona USA) or fluoride alone (NUPRO White, Dentsply Sirona USA) using fluoride-Ion Selective Electrode (F-ISE), Inductively Coupled Plasma-Optical Emission Spectroscopy (ICP-OES), X-Ray Diffraction (XRD), Fourier Transform Infrared Spectroscopy (FTIR), ^{19}F and ^{31}P Magic Angle Spinning-Nuclear Magnetic Resonance (MAS-NMR).

Methods. A thin layer (0.0674±0.0005 g) of each varnish (20×25 mm in area) was spread on a roughened glass slide (n=7). They were separately immersed in 10 ml Tris buffer (0.06M, pH=7.30), and changed after 1, 2, 4, 6, 24 and 48 hrs. Fluoride-ion concentration at each time using the F-ISE, whilst calcium and phosphate release were investigated using ICP-OES. XRD, FTIR. MAS-NMR analyses were also performed before and after immersion.

Results. The cumulative F-ion release was significantly higher in CPP-ACPF (1.113 mmol/g)>BGAF(0.638)>F(0.112) (p<0.001). The cumulative calcium and phosphorus were higher in the CPP-ACPF (0.137 mmol/g, 0.119) than BGAF (0.067, 0.015) (p<0.001) respectively. The XRD and ^{19}F MAS-NMR confirmed the presence of NaF peaks in all cases before immersion. There were less prominent signal and appearance of fluorapatite crystals after immersion. ^{19}F MAS-NMR revealed CaF_2 formation after immersion in both CPP-ACPF and BGAF. ^{31}P MAS-NMR showed phosphate signals in both CPP-ACPF and BGAF before immersion. FTIR failed to show any signs of apatite formation.

Significance. Both CPP-ACP and bioactive glass enhanced ion release without compromising the bioavailability of fluoride. The CPP-ACPF varnish had the most promising ion release.

A Comparative Evaluation of Ion Release Characteristics of Three Different Dental Varnishes containing Fluoride either with CPP-ACP or Bioactive glass

Ahmed Sleibi, Tappuni AR, Natalia G. Karpukhina, Robert G. Hill, Baysan A

Ahmed Sleibi (corresponding author)
Institute of Dentistry, Queen Mary University of London, Turner Street, EI 2AD, London, United Kingdom
Email: dr_ahmedsm75@yahoo.com

Anwar R. Tappuni
Institute of Dentistry, Queen Mary University of London, Turner Street, EI 2AD, London, United Kingdom

Natalia G. Karpukhina
Dental Physical Sciences Unit, Institute of Dentistry, Queen Mary University of London, Mile End Road EI, 4NS, London, United Kingdom

Robert G. Hill
Dental Physical Sciences Unit, Institute of Dentistry, Queen Mary University of London, Mile End Road EI, 4NS, London, United Kingdom

Aylin Baysan
Institute of Dentistry, Queen Mary University of London, Turner Street, EI 2AD, London, United Kingdom

Introduction

Dental varnishes containing fluoride have increasingly been used to manage dental caries in different age groups, with special emphasis on high-risk individuals [1], [2], [3], [4], [5], [6]. However, the efficacy of fluoride alone is limited by the bioavailability of calcium and phosphate especially in compromised situations i.e., patients with xerostomia [7]. This is the rationale for incorporating different calcium phosphate formulations such as casein phospho-peptide-amorphous calcium phosphate (CPP-ACP), and more recently bioactive glass (calcium sodium phospho-silicate, BGA), since the availability of fluoride in the oral cavity with the presence of these ions can inhibit the demineralisation process, through the substitution of the hydroxyl ion of the hydroxyapatite [$Ca_5(PO_4)_3(OH)$] by the fluoride ion forming fluorapatite [$Ca_{10}(PO_4)_6F_2$] [8]. The newly formed crystals can then make the tooth structure more resistant to dental caries [9], [10].

Superior results were reported using sources of calcium and phosphate either with [7] or without fluoride in dentifrices and mouthwashes [11], when compared with fluoride alone for the prevention of dental caries in adult populations. It can be suggested that the delivery of a combination of these ions could be also required in best scenario when both calcium and phosphate are freely available in oral fluids. This is probably due to the application of a dental varnish containing fluoride alone on the demineralised area which might act as a physical barrier. The ingredients of dental varnish consist of different adhesive and non-active ingredients that could restrict calcium and phosphate ion penetration from the oral fluids and prevent the subsequent combination with fluoride to enter the subsurface lesion layers. Since the level of salivary flow rate diminishes significantly at night [12], this would restrict the salivary calcium and phosphate availability to the tooth surface and therefore would reduce the potential rate of remineralisation of saliva on tooth structure.

In contrast to dental varnishes containing fluoride alone, fluoride could combine with calcium to form either calcium fluoride (CaF_2) or ‘calcium fluoride-like’ (CaF^+) composition in the presence of CPP-ACP and fluoride [13], whilst low soluble fluorapatite could be formed in the presence of phosphate restricting the bioavailability of free fluoride ion [1], [14], [15]. This would ultimately affect the remineralisation process. Though, the presence of peptide in the CPP-ACP formula might aid in stabilising fluoride, calcium and phosphate, and

prevent the combination of these ions [16], [17]. It has been reported that in a laboratory setting, a dental varnish containing CPP-ACP and fluoride demonstrates the highest fluoride and calcium ion release compared with other calcium phosphate formulations and fluoride alone varnishes over a period of 48 h [18], [19]. In a recent systematic review, combination of fluoride and CPP-ACP had an optimum remineralisation efficacy on enamel lesions when compared with a fluoride alone treatment [20].

Alternatively, the introduction of BGA within a fluoride varnish formulation is a relatively a new approach that has not yet been investigated extensively. BGA is a ceramic material comprising of amorphous sodium-calcium-phosphosilicate that is highly reactive in water [21]. Following the BGA immersion in an aqueous solution, calcium, sodium, and phosphate ions are expected to be released. This permits the ionic exchange of Na^+ with H^+ or H_3O^+ at the glass-liquid interface, allowing the formation of a supersaturated ionic reservoir. The silanols that result following BGA dissolution act as a nucleation site to form an apatite structure by attracting the released calcium and phosphate ions, forming a calcium phosphate rich layer [22], [23]. In previous *in vitro* studies, there was evidence that using BGA will enhance the remineralisation process in both enamel and dentine [24], [25], [26].

Despite the current efforts to develop a dental material that can achieve a sustained platform of ion release without potential antagonistic reaction that affects their bioavailability, there are lack of studies that have assessed the kinetic ion release of a novel BGA containing fluoride varnish that have different chemical composition and physical behaviours on enamel and dentine. Therefore, the aim of this laboratory based study was to compare the ion release characteristics of three different dental varnishes containing fluoride either with CPP-ACP or BGA and fluoride alone, using the F-ISE, ICP-OES, XRD, FTIR, ^{19}F MAS-NMR and 31P MAS-NMR.

2. Methodology

2.1. Dental varnish groups

Three commercial dental varnishes formulated with fluoride (5%NaF WT) and CPP-ACP, fluoride (5%NaF WT) and BGA, or fluoride alone (5%NaF WT) were investigated to assess fluoride, calcium, and phosphate ion release (Table 1). The study flow chart is illustrated in Figure 1.

2.2. Tris buffer preparation

The Tris buffer (0.06 M) was prepared by dissolving 15.090 g tris-(hydroxymethyl) aminomethane (Sigma–Aldrich) in 800 ml deionised water at room temperature. Then, 44.2 ml of 1 M hydrochloric acid (Sigma–Aldrich) was gradually added to the solution. This was left at 37°C in a shaker overnight. 1 M hydrochloric acid was used to adjust the pH to 7.30 at 37°C using Oakton pH meter (Oakton Instruments, Nijkerk, The Netherlands). Deionised water was added to the prepared solution up to a total volume of 2000 ml. The tris buffer was kept in an incubator at 37°C, and the pH was re-measured prior to the sample immersion [27]. The pH meter was calibrated during the study time with standard pH buffer solutions pH 4.01, 7 and 10.01 (Oakton meters for pH, Vernon Hills, IL, USA).

2.3. Powder extraction from the commercial varnishes

50 mg of varnish from a newly opened package was placed inside a 1.5 ml centrifuge tube with a lid on the top (Eppendorf, Dutscher Scientific Ltd. Essex, UK), and 1.0 ml of acetone (≥99.5%, VWR International France) was added, and closed the lid. Subsequently, the tube was shaken vigorously by hand for approximately 1 min to initiate extraction of the powder and separation of acetone soluble components. The sample was then left for 30 min to allow the first solid fraction to sediment on the tube. The liquid above the sediment was carefully transferred (suctioned dispensed) using a small pipette (3 ml, Sigma-Aldrich, Gillingham, Dorset, UK). The solid sediment was undergone the same procedure with 1.0 ml acetone extraction again. The solid fractions of the powder were collected and left for 24 h at room temperature to dry, then for another 24 h on top of a drying oven (50°C) to evaporate the acetone remnants. The obtained

dried materials that were extracted from each dental varnish ended up as white powder. This powder was then analysed using the XRD, FTIR and NMR to assess the characteristics of each varnish characteristics before the immersion in tris buffer.

2.4. Sample preparation for ion release in tris buffer

Plastic microscope slides with rough surfaces (VFM, CellPath Ltd, Powys, UK) were used to spread each test varnish on an area of 20×25 mm. These slides were weighed before and after the varnish application to ensure each slide received the same amount of dental varnish. The lid of each varnish package was removed and content was mixed using clean small brush (provided with MI varnish brush, GC, Japan) to ascertain that active and inactive contents were spread evenly. Subsequently, a thin layer of dental varnish was painted on the allocated area using another clean small brush for each sample being 0.0674±0.0005 g in weight. A total of seven samples were prepared for each group, and these samples were individually immersed in 10 ml of tris buffer. The varnish was applied immediately following the opening of varnish sachet to reduce any possible weight change due to any possible evaporation of the volatile components such as ethanol. After application of the varnish to the substrate they were kept in a shaking incubator (60 rpm agitation, KS 4000 IKA, UK) incubator at 37°C in 10 ml of tris buffer. These samples were then removed from the tris buffer solution and placed in a new plastic vial containing a further 10 ml tris buffer after 1, 2, 4, 6, 24 and 48 h. The immersion solution was individually assessed to investigate fluoride, calcium and phosphate ion release at 1, 2, 4, 6, 24 and 48 h.

The F-ISE (Orion 9609BNWP, Thermo Fisher, USA) was calibrated at room temperature using the solutions with 5, 50, and 100 ppm fluoride. The calibration plot, the potential (E, mV) versus Lg ([F], mol/L), was linear and had a slope that was within the range of −59 to −60 mV *per* decade [F−] mol/l. Following this calibration, fluoride ion concentration was measured for all groups at each time point using the same Electrode F-ISE.

Based on nominal percentage of NaF in the varnish and taking into account the experimental manipulations with each sample, the estimated maximum amount of fluoride ions that can be released throughout the 48 h in 60 ml tris buffer were calculated. The total fluoride (ppm) release was then deducted to estimate the potential remaining amounts of fluoride ion in the varnish samples after each immersion.

The same immersion solutions were analysed to measure the concentration of calcium, and phosphate at each time point using an Inductively Coupled Plasma-Optical Emission Spectroscopy (ICP-OES, Vista-PRO Oxford, UK).

2.5. X-Ray Diffraction (XRD)

X-ray diffraction was performed on the varnishes before immersion to detect the presence of crystalline NaF and after immersion to detect the loss of NaF and the possible formation of crystalline fluorapatite and calcium fluoride.

XRD analyses were carried out for the extracted powder before immersion and the powder after the immersion was also investigated. These measurements were calculated using an X'Pert Pro X-ray diffractometer (PANalytical, The Netherlands). Data collected at room temperature with a 0.033° 2θ step size and a count rate of 99.6 s step−1, from 2θ values of 10° to 70°). Each sample collected after 48 h immersion were left for 72 h at room temperature to be dried, and analysed with the same procedure. XRD patterns obtained for each tested varnish were compared against the reference patterns of hydroxyapatite (Reference code: 01-073-6113), NaF (00-036-1455), and TiO_2 (04-013-5313, 04-003-0844, and 04-003-0648).

2.6. Fourier Transform Infrared Spectroscopy (FTIR)

The FTIR (Spectrum GX, Perkin-Elmer, Waltham, MA, USA) analysis was performed on the liquid varnish samples prior to the immersion, and varnish powder after 48 h of tris buffer immersion was tested using the FTIR. Data was collected from 1750 to 500 cm^{-1} wavenumbers. The FTIR analysis was also carried out on a pure NovaMin (Bioglass® 45S5) sample for reference purposes.

2.7. Magic Angle Spinning-Nuclear Magnetic Resonance Spectroscopy (MAS-NMR)

MAS-NMR was performed on the varnishes before and after immersion to investigate the chemical speciation of phosphorus and fluorine in the varnish. The integrated area under the NMR peak is proportional to the amount of the species present. In addition ^{19}F MAS-NMR unlike XRD enables fluorapatite to be distinguished from hydroxyapatite. The varnish samples before and after the immersion were analysed using the MAS-NMR spectroscopy (Bruker, Germany). Solid-state MAS-NMR experiments were carried out using the 600MHz Bruker spectrometer with the magnetic field of 14.1 Tesla. The ^{19}F and ^{31}P MAS-NMR spectra were collected at the resonance frequencies of 564.7MHz and 242.9MHz respectively. The sample was packed in 2.5mm o.d. zirconia rotor and spun at 20 kHz using the standard double resonance Bruker probe with low fluorine background. 1M aqueous solution of NaF producing a sharp signal -120ppm was used to reference ^{19}F chemical shift scale. 85% H3PO4 was used to reference the ^{31}P chemical shift scale. All experiments were run with 60 seconds recycle delay.

2.8. Statistical analysis

The differences in ion release at each time point and cumulatively among the test varnishes were statistically analysed using the repeated measurements of ANOVA and pairwise comparisons. Data analyses were performed using IBM SPSS Statistics 24.0 (SPSS Inc., Chicago, IL, USA). Sample size calculation was based on the data from a previous study [18]. The statistical power was set to 85% at a level of significance of 0.05 (two sided)

3. Results

3.1. Fluoride ion release

The initial fluoride release at 1 h of immersion was significantly higher for the CPP-ACPF varnish (0.593 mmol/g) compared to BGAF (0.187 mmol/g), and F (0.025 mmol/g) (p<0.001). However, F ion release was higher at 24 h immersion time point for both BGAF and F varnishes when compared to the CPP-ACPF

varnish, with the values reaching 0.214 mmol/g (p<0.001), mmol/g, 0.0475, and 0.030 mmol/g respectively (Figure 2).

Cumulatively, the CPP-ACPF varnish showed the greatest fluoride ion release (1.113 mmol/g) when compared to both BGAF (0.638 mmol/g), and F alone (0.112mmol/g) varnishes across the 48 h immersion period (p≤0.001). However, there was a significant increase in the trend of ion release for the BGAF (p≤0.001), and slight increase for the F alone varnish at 6-48 h time interval when compared to the CPP-ACPF. Both CPP-ACPF and BGAF cumulative F ion release showed deviations from the square root time at later times compared with the F alone varnish (Figure 3). The expected total amount of fluoride ion in each varnish sample that was available to be released in 60 ml of tris buffer was 1.775 mmol/g in all cases. There was a difference in the rate of fluoride release among the test varnishes, the CPP-ACPF exhibited the fastest fluoride release, followed by the BGAF and the F alone varnish gave the slowest release (Figure 4).

3.2. Calcium and phosphate ion release

The highest initial burst of both calcium and phosphate ions was for the CPP-ACPF varnish, 0.0295 and 0.0516 mmol/g, compared to the BGAF varnish, 0.006 and 0.001 mmol/g respectively. The second burst in calcium ion release for both varnishes was at 6-24 h interval then a decreasing in release was observed for the remaining time period (Figure 5).

Over the 48 h, the CPP-ACPF varnish showed a significant increase in both calcium and phosphate cumulative ion release in comparison to the BGAF varnish (p<0.001). Both varnishes showed more calcium ion release after the 6 h time point immersion when compared to phosphate ion release. Deviation of the cumulative calcium and phosphate ion release from the square root time dependence at later times was identified for the CPP-ACPF varnish only (Figure 6).

Both CPP-ACPF and BGAF varnishes showed differences between the theoretical Ca:P ratio that would be expected for either CPP-ACP or NovaMin, and the measured Ca:P ratios in this study. The theoretical Ca:P ratio for ACP/CPP would be between 1.3 and 1.5 and the experimental values were lower than the minimum of 1.3. The theoretical Ca:P ratio for NovaMin should be about 5.2, whilst the Ca:P values of the BGAF started at 3.44 at 1h and increased to 4.56 at 48 h. (Figure 7).

3.3. X-Ray Diffraction (XRD)

The XRD pattern of each sample before immersion revealed several strong diffraction lines (filled black circles) at 38.7°, 56.0° and minor at 33.5° and 67.0° 2θ, all of which correspond to crystalline NaF (Figure 8). Another two minor diffraction lines at 29.0° and 35.0° were not identified. The XRD pattern of each sample after immersion failed to show significant diffraction lines for NaF and revealed the substantial presence of an amorphous phase with a broad diffraction halo at around 16° 2θ and second halo at around 22° 2θ. Two minor diffraction lines at 10.8° and 15.4° 2θ were present, but not identified.

The XRD patterns of BGAF varnish before and after immersion are illustrated in Figure 9. The pattern revealed diffraction lines at 38.8°, 56.1°, 33.5° and 67.0° 2θ confirming the presence of NaF in the sample before immersion. The lines became less pronounced after 48 hrs of immersion. Additional diffraction peaks at 25.4°, 37.9° and 48.1° 2θ corresponding to a titanium dioxide (anatase) a whitening agent were seen in the sample before immersion. TiO_2 remained after the immersion based on the diffraction line at 25.4° 2θ still being present (ii) in Figure 9. A small broad hump is seen around 30° 2θ in the sample before immersion was similar to the broad amorphous halo of the 45S5 glass powder (Figure S2 supporting information), which identified the presence of unreacted bioactive glass powder in the varnish sample. The original broad halo disappeared after immersion in the test sample and a much broader and asymmetric hump appeared with the centre between 15° and 22° 2θ. A number of sharp, though relatively minor, diffraction lines can also be seen at 16.1°, 16.7° and 14.3° 2θ in addition to a small diffraction line at 10.8° 2θ in the pattern.

The XRD pattern of the fluoride alone varnish in Figure 10 before immersion showed the diffraction lines at 38.8°, 56.1°, 33.5° and 66.9° 2θ corresponding to NaF, NaF. Only two major diffraction lines 38.7° and 56.1° 2θ remained in the pattern of the sample after 48 hrs tris immersion. The sample before immersion also showed the presence of titanium dioxide phase revealed by the presence of the diffraction lines at 25.3°, 37.7° and 48.1° 2θ. The sample after immersion showed a number of unidentified relatively strong diffraction lines at the positions of 16.0°, 16.7°, 14.3°, 8.4° and 10.8° 2θ. These diffraction lines were similar to those seen in the patterns of the immersed samples of two other varnishes (Figures 8&9) and therefore this might possibly be originating from partially crystallised hydrogenated rosin during immersion. It can also be seen that there was a broad amorphous halo pattern at around 16° 2θ in the immersed sample, which was quite close to the supressed broad intensity in the sample before immersion around the same 2θ values.

3.4. *Magic Angle Spinning-Nuclear Magnetic Resonance Spectroscopy (MAS-NMR)*

Figure 11 showed the ^{19}F MAS-NMR spectra of varnish samples before the immersion. The main signal seen in all spectra was relatively sharp line at about -225ppm. Thus, all the ^{19}F MAS-NMR spectra showed dominant presence of fluorine present as crystalline NaF. Since the dominance of the -225 pm signal was overwhelming, the spectra of the two samples with CPP-ACP and with bioactive glass were zoomed to reveal any other details in addition to the strong fluorine signal corresponding to NaF. From the spectra i and iii in Figure 11, there was a weak signal at between -104 and -105 ppm, which corresponded to a partially fluoride substituted apatite. The substitution by fluoride was partial and crystallinity of this apatite was low based on the position and linewidth of the signal.

Figure 12 shows the ^{19}F MAS-NMR spectra of the varnish samples collected after immersion. After 48 hrs tris immersion, the ^{19}F MAS-NMR spectra of both BGAF (ii) and F alone (iii) varnishes showed the dominant presence of the fluorine-19 signal at around -225 ppm, which corresponded to the fluoride from the crystalline NaF. This signal was much less prominent in the spectrum of the CPP-ACPF varnish (i). All three spectra also contained a peak at around -109 ppm. This was close to the signal of fluoride in crystalline calcium fluoride CaF_2.

The ^{31}P MAS-NMR spectrum of the CPP-ACPF varnish (i, top spectrum in Figure 13) showed a single relatively broad peak at about 3 ppm. The BGAF varnish before immersion presented a broad feature at 8.4 ppm, and small sharp signal at about 2.2ppm (ii, bottom spectrum in Figure 13).

The ^{31}P MAS-NMR spectra of the CPP-ACPF and BGAF varnishes failed to show a signal following the immersion as seen in Figure 14. This meant no phosphorus species were left in these varnishes after the immersion.

4. Discussion

It was worth noting that all three varnishes had the same total NaF content. Thus, the different kinetics of release are due to the additional component (CPP-ACP/bioactive glass) and/or the different resins used. The maximum ion release was for the CPP-ACPF followed by BGAF, and F varnish had the lowest release. Both calcium phosphate based varnishes are a source of bioavailable fluoride, calcium and phosphate ion. Tris buffer was used in the current study as an immersion solution to investigate the ion release behaviour, rather than the simulated body fluid or artificial saliva that would more closely mimic the natural saliva. This was to exclude the effect of the additional calcium and phosphate from these fluids, which may camouflage the potential ion release from the test materials [28], [29]. The immersion solution was changed at each time point to simulate the effect of saliva exchange as *in vivo* condition and ion measurement was performed. Studying ion release with a longer time of immersion, more than 48 h, wasn't considered in this study, due to the fact these dental varnishes would be unlikely to be retained on tooth surface for much longer than this time period due to the potential removal during mastication and by salivary fluids. It was reported that retention of dental varnishes are limited in the oral cavity for only several hours following application [1].

In this study, a uniform film thickness of varnish was achieved by applying an equal amount of varnish spread over a standardised area to minimise sample to sample variations that would influence the ion release. In

addition, the samples were promptly applied to the substrate to reduce the possible change in varnish weight as a result of evaporating the volatile constituents such as isopropanol and ethanol that might affect ion load percentage in each sample.

4.1. Fluoride

The highest initial burst of fluoride together with the maximum total amount of fluoride released over 48 h was for the CPP-ACPF varnish, could be related to the differences in their chemical composition, and physical properties, including resin type, density, viscosity, and particles size [30], [31], [32]. Water sorption and solubility of dental materials have a significant impact on their performance, since water could encourage a range of chemical and physical processes that influence the structure and function of the material itself [33]. It was reported that dissolution time of polyvinyl acetate (PVA) as a water soluble polymer was relatively short [34], and the maximum burst was in the first hour of immersion [35], which was consistent with the trend of fluoride ion release from the CPP-ACPF varnish. PVA has a higher ability to blend due to its polarity and CO2 affinity amongst other proposed polar structures. The interaction between the residual carbonyl groups on the polar gases, such as CO2, and the morphological changes possibly would increase solubility [36], [37]. In this respect, the PVA solubility is substantially increased in the presence of organic solvents [38]. Therefore, it can be suggested that the presence of PVA in addition to ethanol within the CPP-ACPF varnish formulation may contribute to a higher dissolution rate and faster ion release compared to other varnishes tested. This result was also consistent with a previous finding that a combination of polyethylene co-vinyl acetate and NaF resulted in a higher initial burst effect and short release time compared with a same formula of varnish plus an additional polyethylene co-vinyl acetate coat [39]. In addition, the presence of ethanol in the CPP-ACPF formula might easily evaporate leaving pores that are likely to facilitate water movement through the varnish [40]. In contrast the presence of isopropanol in both BGAF and F varnishes t is less likely to evaporate compared to the ethanol [41]. In a recent study, it was reported that the CPP-ACPF varnish has small and homogenous particles, facilitating ion release compared with both BGAF and F varnishes that have large particles (unpublished data, Operative Dentistry) (Figure S1). These authors suggested that the large particles may take longer to dissolve in the immersion solution.

The lowest initial burst and cumulative fluoride ion release for both BGAF and F varnishes might also be related to the presence of Urethane methacrylate resin in their compositions. This resin is less soluble and has a lower water sorption, [42], [43], which would be expected to result in less ion release and this was observed throughout this study. Therefore, both these varnishes are less likely to take up water to swell, dissolve and subsequently to release ions, which could explain the retained substantial amount of fluoride ions retained particularly for the varnish containing fluoride alone. In addition, the burst release was lower for the BGAF and undetected for the F varnish when compared to the CPP-ACPF formula with the PVA resin.

The other possible cause for this variation in fluoride release between the test varnishes could be related to the high solubility of CPP-ACP complex in aqueous solution [44], which might enhance the dissolution of NaF particles in the immersion buffer. This was supported by previous findings where the CPP-ACPF gave the highest fluoride ion release compared to different calcium phosphate formulations and fluoride alone varnishes [18], [19]. Mehta (2014) [45] reported that CPP-ACP was unlikely to adhere to the tooth surface due to its amorphous nature when compared to the firmly attached bioactive glass particles [38], [42], [43].

The BGAF had a higher fluoride release compared to the varnish fluoride alone. This could be due to the ability of BGA to release calcium, sodium, and phosphate in an aqueous solution. This permits for an ionic exchange of Na^+ for H^+ or H_3O^+ at the glass-liquid interface, allowing the formation of saturated ionic reservoir in the immersion solution [22]. This potentially allows the varnish to dissolve following the tris immersion by releasing more fluoride compared to the F alone varnish. However, both BGAF and F varnishes, excluding the initial burst at 1 h time point, showed the same burst of F release that started at 6 h time point and the maximum release was at 24 h. This could be due to both varnishes having the same additives, including the type and the percentage of the carrier resin. The existence of urethane methacrylate in both varnishes that is unlikely to swell, again would delay the burst effect compared to the PVA effect in the CPP-ACP formulation.

The cumulative ion release were plotted in a square root time dependence at early times and indicates a linear relationship indicative of a diffusion controlled mechanism. However at later times they may deviate from linearity. At longer times the fluoride release for the CPP-ACPF varnish no longer had a square root time dependence. This was possibly because most of the fluoride has been released. The BGAF varnish also exhibited this effect but it occurred at longer times because of the slower fluoride release. This effect was not observed for the F varnish which exhibited a square root time dependence till the longest time point studied (Figure 3).

Interestingly, the results from the XRD supported the findings of ion release. The amount of NaF crystals at the baseline before the immersion was high in all varnishes. Whilst after 48h immersion there was no NaF left in the CPP-ACPF and seemed to be unclearly detected in CPP-ACPF, identified in BGAF, and more apparent in the F alone varnish after 48 h immersion.

The ^{19}F MAS-NMR spectra of the varnish powders confirmed the dominant nature of fluorine in all cases before the immersion (Figure 11). The detection of fluorapatite crystals even in small amounts in the samples powder of CPP-ACP and BAGF before immersion may be due to; i) the reaction of varnish ingredients within the varnish container, or ii) it could be due to reaction and crystallization during the extraction process during powder preparation. The amount of fluorapatite detected in the CPP-ACP powder is much smaller than with the BGAF powder. The presence of the peptide αS1-CN (59–79) in the CPP-ACP structure might potentially aid in stabilising fluoride, calcium and phosphate in an aqueous solution in the pH range of 6-9 thereby preventing calcium phosphate and fluoride ions forming fluorapatite [16], [17].

With time, the amount of NaF reduced in the varnishes. This was most marked for the CPP-ACPF that released the most fluoride whilst XRD detected no crystalline NaF a very small amount is present in the 19F spectrum with a chemical shift at -225ppm. In addition there is a small amount of CaF2 present with a chemical shift at -108ppm within the varnish. There was no evidence of fluorapatite forming that would exhibit a peak at -103ppm. This was supported by the absence of a peak for apatite in the ^{31}P spectra after

immersion. The BGAF had a similar behaviour but there was much more NaF left in the varnish at 48 h. Again there was no evidence of any fluorapatite forming in the varnish. This was also supported by the absence of a signal for apatite at about 3ppm in the ^{31}P spectra. The F alone varnish exhibited the strongest NaF signal at 48 h. Neither CaF_2 nor fluorapatite could be formed due to the lack of calcium and phosphate. This varnish released the least cumulative amount of fluoride at 48 h which is in agreement with the large amounts found after immersion by NMR and XRD.

The detection of CaF_2 in the CPP-ACPF reported in this paper following the immersion, however not before the immersion, could be due to the presence of the active sequence –Ser(P)-Ser(P)-Ser(P)-Glu-Glu- in the CPP-ACP formulation that has a remarkable effect in stabilising calcium and phosphate as nanoclusters of ions in metastable solution [46]. This allows the CPP to bind to forming nanoclusters of calcium and phosphate ions to form nanocomplexes of approximately 1.5 nm radius, inhibiting their growth to the critical size required for nucleation and phase transformation [47]. This complex is highly soluble in water releasing their ions that can combine with fluoride to form CaF_2. Similarly, the BGA can commence the ion exchange following the contact with an aqueous solution [Hench 1998]. The CaF_2 is very insoluble [48]. Thus, this compound can be precipitated or formed on the varnish surface following the immersion, and detected by the NMR spectra.

Based on the nominal content of fluoride and the expected total amount of fluoride that should be released from each varnish sample in 60 ml of tris buffer (1.775 mmol/g), the CPP-ACPF approximately released more than 62.7% of the total amount of F in sample varnish, BGAF 35.9%, and F 6.3%. Accordingly, CPP-ACPF varnish released most of its fluoride content following the immersion, whilst both BGAF and F varnishes retained more fluoride ions and clearly the release possibly would therefore be longer for these two varnishes. Nevertheless, the percent of ion release would not completely reflect the actual released amount as both F-ISE can detect the free ion only and is not capable of detecting fluoride in the CaF_2 and fluorapatite crystals.

4.2. Calcium and phosphate

The initial burst of calcium and phosphate release was higher for the CPP-ACPF when compared to the BGAF. It can also be speculated that this variation could be related to their chemical compositions and physical properties [30], [31], [32]. The total amount of both calcium and phosphate released from the CPP-ACPF was higher than the BGAF varnish. This was probably due to the amount of calcium and phosphate being much higher in the CPP-ACP complex compared to the BGA. Calcium and phosphate are the major constituents of the CPP-ACP whilst the BGA 45S5 is composed of 46.1 SiO_2, 2.6 P_2O_5, 24.4 Na_2O and 26.9 CaO (mol%) [49]. In both varnishes, the amount of calcium released was higher than the amount of phosphate. This might also be related to the variation in Ca:P ratio in their compositions approximately 3:2 and 10:1 for the CPP-ACP and BGA respectively [17], [49]. The difference in Ca:P ratio was clearly seen in 24 h time point of both CPP-ACP and bioglass varnishes, where the maximum release of calcium in both varnishes was much greater than P (Figure 5).

The high calcium ion release from the CPP-ACPF was also revealed in previous studies compared to fluoride varnishes, either with modified tricalcium phosphate (Clinpro White, 3M ESPE, MN, USA), dibasic sodium phosphate and calcium sulfate dihydrate (Enamel Pro, Premier Dental Products, PA, USA), calcium fluoride (Bifluorid 5 Voco, Cuxhaven, Germany), or fluoride alone (Duraphat Colgate Oral Care, NSW, Australia) [18]. The bioavailability of calcium and phosphate ions in the CPP-ACP formula in addition to the high solubility of the complex in water might be a reason for the differences in quantity and time of calcium release [18], [44].

The difference between the theoretical ratio and the experimental ratio for both the CPP-ACPF and BGAF that was shown in this study (Figure 7) could be due to the formation of CaF_2 that was seen to form in the ^{19}F Spectra (Figure 12). The formation of CaF_2 would consume calcium and reduce the Ca:P ratio.

The general trend of calcium and phosphate release of the BGAF varnish was almost comparable to the F release and reflecting the ability of this varnish to release ions not only for the first 6 h time point immersion but also for the following hours compared to the CPP-ACPF which released most of its ions earlier at the 1-6 h time point. This could again be related to the type of carrier used in the varnish, Urethane dimethacrylate that will not dissolve by water [42], [43]. However, the CPP-ACPF varnish showed an increase in calcium

release at 6 h immersion following the dramatic decrease in the first 6 h which was inconsistent with the continuous decrease in fluoride release. This could be related to the consumption of a significant fraction of the calcium ions by the formation of CaF_2 in the first 6 h, whilst after 6 h time point, the amount of fluoride was insufficient to consume total amount of free calcium ion. Therefore, this explains the dramatic increase in calcium ion concentration in the immersion solution. The difference in the quantity of calcium/phosphate released at 24 h was also noticed in the BGAF varnish. This could again be the long immersion period, time point 6 to 24 h, that would consume most of the released fluoride to form CaF_2 leaving the calcium ion free in the immersion solution that can be detected by ICP-OSE. The variation in Ca:P ratio in the structure of both CPP-ACP and BGA would be another reason for this difference.

The ^{31}P MAS-NMR confirmed the presence of phosphate in both CPP-ACPF and BGAF varnishes before immersion, however it was not present after 48 h, this implies all the phosphorus was released.

The FTIR spectra supported that the type of BGA in the BGAF varnish was 45S5 (Figure S2). There was no sign of apatite formation detected after 48h h tris immersion in the test varnishes (Figure S3-S5). This was consistent with the NMR results.

5. Conclusion

This laboratory based study demonstrated there was for CPP-ACPF and BAGF varnishes tested to provide fluoride bioavailability in addition to calcium and phosphate. The dental varnish containing CPP-ACP and fluoride released more ions (Ca, P and F) when compared to the bioactive glass varnish, whilst the fluoride alone varnish appeared to retain fluoride longer over the study period. The variation in chemical compositions of inactive ingredients and/or calcium phosphate system influences the dynamics of ion release, regardless of fluoride content. This is of clinical value regardless of the releasing time (short/long) and could be considered to potentially enhance the remineralisation process, both on enamel and dentine.

References

1. Beltrán-Aguilar ED, Goldstein JW, Lockwood SA. Fluoride varnishes. A review of their clinical use, cariostatic mechanism, efficacy and safety. J Am Dent Assoc, 2000; 131:589-596.
2. Azarpazhooh A and Main PA. Fluoride varnish in the prevention of dental caries in children and adolescents: a systematic review. J Can Dent Assoc, 2008; 74:73–9.
3. Ekstrand K, Martignon S and Holm-Pedersen P. Development and evaluation of two root caries controlling programmes for home-based frail people older than 75 years. Gerodontology, 2008; 25 (2):67-75.
4. Gibson G, Jurasic MM, Wehler CJ and Jones JA. Supplemental fluoride use for moderate and high caries risk adults: a systematic review. J Public Health Dent, 2011; 71 (3):171–84.
5. Karabekiroglu S. S and ˘ Unl¨u N. Effectiveness of different preventive programs in cariogram parameters of young adults at high caries risk. Int J Dent, 2017; 7189270:1-10.
6. Rossa Al, Sherriff A,Kidd J, Gnich W, Anderson J, Deas L and Macpherson L. A systems approach using the functional resonance analysis method to support fluoride varnish application for children attending general dental practice. Appl Ergon, 2018; 68:294–303.
7. Papas A, Russell D, Singh M, Stack K, Kent R, Triol C et al. Double Blind Clinical Trial of a Remineralizing Dentifrice in the Prevention of Caries in a Radiation Therapy Population. Gerodontology, 1999; 16(1):2-10.
8. Reynolds E. Calcium phosphate-based remineralization systems: Scientific evidence? Aust Dent J, 2008; 53(3):268-273.
9. Ten Cate J.M and Featherstone J.D.B. Mechanistic aspects of the interactions between fluoride and dental enamel. CRC Crit Rev Oral Biol Med, 1991; 2(2):283-296.
10. Ten Cate J.M. Review on fluoride, with special emphasis on calcium fluoride mechanisms in caries prevention. Eur J Oral Sci, 1997; 105:461-465.
11. Hay KD and Thomson WM. A clinical trial of the anticaries efficacy of casein derivatives complexed with calcium phosphate in patients with salivary gland dysfunction. Oral Surg Oral Med Oral Pathol Oral Radiol Endod, 2002; 93:271–275.

12. Dawes C. Physiological Factors Affecting Salivary Flow Rate, Oral Sugar Clearance, and the Sensation of Dry Mouth in Man. Journal of Dental Research, 1987; 66(2 suppl):648-653.
13. Vogel G.L. Oral fluoride reservoirs and the prevention of dental caries. M.A.R. Buzalaf (Ed.), Fluoride and the Oral Environment. Monogr Oral Sci. Basel, Karger; 2011; 22:146–157.
14. Ericsson Y. Fluorides in dentifrices. Investigations using radioactive fluorine. Acta Odontol Scand, 1961; 19:41–77.
15. Benzian H, Holmgren C, Buijs M, van Loveren C, van der Weijden F and van Palenstein Helderman W. Total and free available fluoride in toothpastes in Brunei, Cambodia, Laos, the Netherlands and Suriname. Int Dent J, 2012; 62:213-221.
16. Reynolds EC, Black CL, Cai F, Cross KJ, Eakins D, Huq NL, et al. Advances in enamel remineralization: casein phosphopeptide-amorphous calcium phosphate. J Clin Dent, 1999; 2:86-88.
17. Cross KJ, Huq NL, Stanton DP, Sum M and Reynolds EC. NMR studies of a novel calcium, phosphate and fluoride delivery vehicle-α(S1)-casein(59–79) by stabilized amorphous calcium fluoride phosphate nanocomplexes. Biomaterials, 2004; 25:5061-5069.
18. Cochrane NJ, Shen P and Yuan Y, Reynolds EC. Ion release from calcium and fluoride containing dental varnishes. Aust Dent J, 2014; 59:100–105.
19. Shen P, Bagheri R, Walker GD, Yuan Y, Stanton DP, Reynolds C, et al. Effect of calcium phosphate addition to fluoride containing dental varnishes on enamel demineralization. Aust Dent J, 2016; 61: 357-365.
20. Tao S, Zhu Y, Yuan H, Tao S, Cheng Y, Li J and He- PloS one L. Efficacy of fluorides and CPP-ACP vs fluorides monotherapy on early caries lesions: A systematic review and meta-analysis. Journals.plos.org, 2018, PLoS ONE 13(4): e0196660. https://doi.org/10.1371/journal.pone.0196660
21. Gjorgievska ES and Nicholson JW. A preliminary study of enamel remineralization by dentifrices based on Recalden (CPP-ACP) and Novamin (calcium-sodium-phosphosilicate). Acta Odontol Latinoam, 2010; 23:234–9.
22. Hench LL. Bioceramics: From Concept to Clinic. J Am Ceramic Soc, 1991; 74(7):1487–1510.
23. El-Wassefy N.A. Remineralizing effect of cold plasma and/or bioglass on demineralized enamel. Dent. Mater, 2017; 36(2):157–167.

24. Fernando D, Attik N, Pradelle-Plasse N, Jackson P, Grosgogeat B and Colon P. Bioactive glass for dentin remineralization: A systematic review. Mat Sci Eng C, 2017; (76):1369-1377.
25. Taha A.A, Patel M.P, Hill R.G and Fleming P.S. The effect of bioactive glasses on enamel remineralization: a systematic review. J Dent, 2017; (67):9-17.
26. Sleibi A, Tappuni AR, Davis GR, Anderson P and Baysan A. Comparison of efficacy of dental varnish containing fluoride either with CPP-ACP or bioglass on root caries: *Ex vivo* study. J Dent, 2018; 73:91-96.
27. Mneimne M, Hill RG, Bushby AJ and Brauer DS. High phosphate content significantly increases apatite formation of fluoride-containing bioactive glasses. Acta BIiomater, 2011; 7:1827-1834.
28. Fagerlund S, Hupa L and Hupa M. Dissolution patterns of biocompatible glasses in 2-amino-2-hydroxymethyl-propane-1,3-diol (Tris) buffer. Acta Biomater, 2013; 9:5400-5410.
29. Kirste G, Brandt-Slowik J, Bocker C, Steinert M, Geiss R and Brauer DS. Effect of chloride ions in Tris buffer solution on bioactive glass apatite mineralization. Int J Appl Glass Sci, 2017; 8:438 –449.
30. Castilllo JL, Milgron P, Kharasch E, Izutsu K and Fey M. Evaluation of the fluoride release from commercially available fluoride varnishes. J Am Dent Assoc, 2001; 132:1389–1392.
31. Shen C and Autio-Gold JT. Assessing fluoride concentration uniformity and fluoride release from three varnishes. J Am Dent Assoc, 2002; 133:176–182.
32. LaTorre G and Greenspan DC. The role of ionic release from NovaMin (calcium sodium phosphosilicate) in tubule occlusion: an exploratory in vitro study using radio-labeled isotopes. J Clin Dent, 2010; 21:72-6.
33. Park J, Ye Q, Topp E, Misra A, Kieweg S.L and Spencer P. Water sorption and dynamic mechanical properties of dentin adhesives with a urethane-based multifunctional methacrylate monomer. Dent Mater, 2009; 25:1569-1575.
34. Kolter K, Wichtner M, Schönherr M and Mittwollen J. Pharmaceutical formulation for producing rapidly disintegrating tablets. US Patent, 2013; abstract no. US8425935B2. https://patents.google.com/patent/US8425935B2/en.
35. Morita R, Honda R and Takahashi Y. Development of oral controlled release preparations, a PVA swelling controlled release system (SCRS). I. Design of SCRS and its release controlling factor. J Control Release, 2000; 63:297-304.

36. Leijtens T , Ding I.K, Giovenzana T, Bloking J.T, McGehee M.D and Sellinger A. Hole transport materials with low glass transition temperatures and high solubility for application in solid-state dye-sensitized solar cells. ACS Nano, 2012; 6:1455-1462.
37. Chen C.L, Teng H and Lee Y.L. Preparation of highly efficient gel-state dye-sensitized solar cells using polymer gel electrolytes based on poly (acrylonitrile-co-vinyl acetate). J. Mater. Chem, 2010; 21:628− 632.
38. Wang L, Zhang H, Wang C and Ma T. Highly stable gel-state dye-sensitized solar cells based on high soluble polyvinyl acetate ACS Sustain. Chem. Eng; 2013; 1:205-208.
39. Baturina O, Tufekci E, Guney-Altay O, Khan SM, Wnek GE and Lindauer SJ. Development of a sustained fluoride delivery system. Angle Orthod, 2010; 80(6):1129-1135.
40. Earl M.S.A, Mount G.J and Hume G.R. The effect of varnishes and other surface treatments on water movement across the glass ionomer cement surface. Australian Dental Journal, 1989; 34(4):326-329.
41. Mülhardt C. Der Experimentator: Molekularbiologie/Genomics. Spektrum Akademischer Verlag Heidelberg. 2009; ISBN 978-3-8274-2036-7 page 38.
42. Delbem A.C.B, Brighenti F.L, Oliveira F.A.L, Pessan J.P, Buzalaf M.A.R and K.T. Sassaki. In vitro assessment of an experimental coat applied over fluoride varnishes. J Appl Oral Sci, 2009; 17:280-283.
43. Ortengren U, Wellendorf H, Karlsson S and Ruyter I.E. Water sorption and solubility of dental composites and identification of monomers released in an aqueous environment. J Oral Rehabil, 2001; 28:1106-1115.
44. Cochrane NJ and Reynolds EC. Casein phosphopeptides in oralhealth. In: Wilson M, ed. Food constituents and oral health: current status and future prospects. Cambridge: Woodhead Publishing Limited, 2009.
45. Mehta AB, Veena Kumari RJ and Izadikhah V. Remineralization potential of bioactive glass and casein phosphopeptide-amorphous calcium phosphate on initial carious lesion: An in-vitro ph-cycling study. J Conserv Dent, 2014; 17(1):3-7.
46. Cochrane NJ, Saranathan S, Cai F, Cross KJ and Reynolds EC. Enamel subsurface lesion remineralisation with casein phosphopeptide stabilised solutions of calcium, phosphate and fluoride. Caries Res, 2008; 42:88–97.

47. Reynolds EC. Casein phosphopeptide-amorphous calcium phosphate: the scientific evidence. Adv Dent Res, 2009; 21:25–29.
48. Øgaard B. CaF2 formation: Cariostatic properties and factors of enhancing the effect. Caries Res, 2001; 35(suppl 1):40-44.
49. Hill R.G and Brauer D.S. Predicting the bioactivity of glasses using the network connectivity or split network models. J Non-Cryst Solids, 2011; 357:3884-3887.

Introduction

Dental varnishes containing fluoride have increasingly been used to manage dental caries in different age groups, with special emphasis on high-risk individuals [1], [2], [3], [4], [5], [6]. However, the efficacy of fluoride alone is limited by the bioavailability of calcium and phosphate especially in compromised situations i.e., patients with xerostomia [7]. This is the rationale for incorporating different calcium phosphate formulations such as casein phospho-peptide-amorphous calcium phosphate (CPP-ACP), and more recently bioactive glass (calcium sodium phospho-silicate, BGA), since the availability of fluoride in the oral cavity with the presence of these ions can inhibit the demineralisation process, through the substitution of the hydroxyl ion of the hydroxyapatite [$Ca_5(PO_4)_3(OH)$] by the fluoride ion forming fluorapatite [$Ca_{10}(PO_4)_6F_2$] [8]. The newly formed crystals can then make the tooth structure more resistant to dental caries [9], [10].

Superior results were reported using sources of calcium and phosphate either with [7] or without fluoride in dentifrices and mouthwashes [11], when compared with fluoride alone for the prevention of dental caries in adult populations. It is suggested that the delivery of a combination of these ions could be required in best scenario when both calcium and phosphate are freely available in oral fluids. This is probably due to the application of a dental varnish containing fluoride alone on the demineralised area, which might act as a physical barrier. The ingredients of dental varnish consist of different adhesive and non-active ingredients that could restrict calcium and phosphate deposition from the oral fluids and prevent the subsequent combination with fluoride penetrate the subsurface lesion layers. Since salivary flow rate shows a circadian rhythm of an amplitude with a drop almost to zero during night, and low rates in summer due to dehydration [12], this would restrict the salivary calcium and phosphate availability to the tooth surface and therefore would reduce the remineralisation potential of saliva on tooth structure.

In contrast to dental varnishes containing fluoride alone, the fluoride in the presence of CPP-ACP could combine with calcium to form either calcium fluoride (CaF_2) or 'calcium fluoride-like' (CaF^+) composition [13], whilst low soluble fluorapatite could be formed in the presence of phosphate restricting the bioavailability of free fluoride ion [1], [14], [15]. This would ultimately affect the remineralisation process. However, the

presence of peptide in the CPP-ACP formula might aid in stabilising fluoride, calcium and phosphate, and prevent the combination of these ions [16], [17]. It has been reported that in a laboratory setting, a dental varnish containing CPP-ACP and fluoride demonstrates the highest fluoride and calcium ion release compared with other calcium phosphate formulations and fluoride alone varnishes over a period of 48 h [18], [19]. A recent systematic review concluded that a combination of fluoride and CPP-ACP had an optimum remineralisation efficacy on enamel lesions when compared with a fluoride alone treatment [20].

The introduction of BGA within a fluoride varnish formulation is a relatively new approach that has not yet been investigated extensively. BGA is a bioactive material comprising of amorphous sodium-calcium-phosphosilicate that is highly reactive in water [21]. Following the BGA immersion in an aqueous solution, calcium, sodium, and phosphate ions are expected to be released. This permits the ionic exchange of Na^+ with H^+ or H_3O^+ at the glass-liquid interface, allowing the formation of a supersaturated ionic reservoir. The silanols that result following BGA dissolution act as a nucleation site to form an apatite structure by attracting the released calcium and phosphate ions, forming a calcium phosphate rich layer [22], [23]. In previous *in vitro* studies, there was evidence that using BGA will enhance the remineralisation process in both enamel and dentine [24], [25], [26].

Despite efforts to develop a dental material that can achieve a sustained platform of ion release without potential antagonistic reaction that affects their bioavailability, there is a lack of evidence in the literature that have assessed the kinetic ion release of a novel BGA containing fluoride varnish that have different chemical composition and physical behaviours on enamel and dentine. Therefore, the aim of this laboratory based study was to compare the ion release characteristics of three different dental varnishes containing fluoride either with CPP-ACP or BGA and fluoride alone, using the F-ISE, ICP-OES, XRD, FTIR, ^{19}F MAS-NMR and ^{31}P MAS-NMR.

2. Methodology

2.1. Dental varnish groups

Three commercial dental varnishes formulated with fluoride (5%NaF WT) and CPP-ACP, fluoride (5%NaF WT) and BGA, or fluoride alone (5%NaF WT) were investigated to assess fluoride, calcium, and phosphorus release (Table 1). The study flow chart is illustrated in Figure 1.

2.2. Tris buffer preparation

The Tris buffer (0.06 M) was prepared by dissolving 15.090 g Tris-(hydroxymethyl) aminomethane (Sigma–Aldrich) in 800 ml deionised water at room temperature. Then, 44.2 ml of 1 M hydrochloric acid (Sigma–Aldrich) was gradually added to the solution. This was left at 37°C in a shaker overnight. 1 M hydrochloric acid was used to adjust the pH to 7.30 at 37°C using Oakton pH meter (Oakton Instruments, Nijkerk, The Netherlands). Deionised water was added to the prepared solution up to a total volume of 2000 ml. The Tris buffer was kept in an incubator at 37°C, and the pH was re-measured prior to the sample immersion [27]. The pH meter was calibrated during the study time with standard pH buffer solutions pH 4.01, 7 and 10.01 (Oakton meters for pH, Vernon Hills, IL, USA).

2.3. Powder extraction from the commercial varnishes

50 mg of varnish from a newly opened package was placed inside a 1.5 ml centrifuge tube with a lid on the top (Eppendorf, Dutscher Scientific Ltd. Essex, UK), and 1.0 ml of acetone (≥99.5%, VWR International France) was added, and closed the lid. Subsequently, the tube was shaken vigorously by hand for approximately 1 min to initiate extraction of the powder and separation of acetone soluble components. The sample was then left for 30 min to allow the first solid fraction to sediment on the tube. The liquid above the sediment was carefully transferred (suctioned dispensed) using a small pipette (3 ml, Sigma-Aldrich, Gillingham, Dorset, UK). The solid sediment was undergone the same procedure with 1.0 ml acetone extraction again. The solid fractions of the powder were collected and left for 24 h at room temperature to

dry, then for another 24 h on top of a drying oven (50°C) to evaporate the acetone remnants. The obtained dried materials that were extracted from each dental varnish ended up as white powder. This powder was then analysed using the XRD, FTIR and NMR to assess the characteristics of each varnish characteristics before the immersion in Tris buffer.

2.4. Sample preparation for ion release in Tris buffer

Plastic microscope slides with rough surfaces (VFM, CellPath Ltd, Powys, UK) were used to spread each test varnish on an area of 20×25 mm. These slides were weighed before and after the varnish application to ensure each slide received the same amount of dental varnish. The lid of each varnish package was removed and content was mixed using clean small brush (provided with MI varnish brush, GC, Japan) to ascertain that active and inactive contents were spread evenly. Subsequently, a thin layer of dental varnish was painted on the allocated area using another clean small brush for each sample being 0.0674±0.0005 g in weight. This was performed using an analytical balance Oxford, accurate to 0.1 mg, (Oxford Instrument Ltd, Oxford, UK) A total of seven samples were prepared for each group, and these samples were individually immersed in 10 ml of Tris buffer. The varnish was applied immediately following the opening of varnish sachet to reduce any possible weight change due to any possible evaporation of the volatile components such as ethanol. After application of the varnish to the substrate they were kept in a shaking incubator (60 rpm agitation, KS 4000 IKA, UK) incubator at 37°C in 10 ml of Tris buffer. These samples were then removed from the Tris buffer solution and placed in a new plastic vial containing a further 10 ml Tris buffer after 1, 2, 4, 6, 24 and 48 h. The immersion solution was individually assessed to investigate fluoride, calcium and phosphorus release at 1, 2, 4, 6, 24 and 48 h.

The F-ISE (Orion 9609BNWP, Thermo Fisher, USA) was calibrated at room temperature using the solutions with 5, 50, and 100 ppm fluoride. The calibration plot, the potential (E, mV) versus Lg ([F], mol/L), was linear and had a slope that was within the range of −59 to −60 mV *per* decade [F−] mol/l. Following this calibration, fluoride ion concentration was measured for all groups at each time point using the same Electrode F-ISE.

Based on nominal percentage of NaF in the varnish and taking into account the experimental manipulations with each sample, the estimated maximum amount of fluoride ions that can be released throughout the 48 h in 60 ml Tris buffer were calculated. The total fluoride (ppm) release was then deducted to estimate the potential remaining amounts of fluoride ion in the varnish samples after each immersion.

The same immersion solutions were analysed to measure the concentration of calcium, and phosphorus at each time point using an Inductively Coupled Plasma-Optical Emission Spectroscopy (ICP-OES, Vista-PRO Oxford, UK). The calcium was measured at 422.673 nm and the phosphorus at 213.618 nm. The calibration range was done at 0-80 ppm. Nitric acid (69%) was added to the samples prior to the measurements to dissolve any particulate materials.

2.5. X-Ray Diffraction (XRD)

X-ray diffraction was performed on the varnishes before immersion to detect the presence of crystalline sodium fluoride (NaF) and after immersion to detect the loss of NaF and the possible formation of crystalline fluorapatite and calcium fluoride.

XRD analyses were carried out for the extracted powder before immersion and the powder after the immersion was also investigated. These measurements were calculated using an X'Pert Pro X-ray diffractometer (PANalytical, The Netherlands). Data collected at room temperature with a 0.033° 2θ step size and a count rate of 99.6 s step−1, from 2θ values of 10° to 70°). Each sample collected after 48 h immersion were left for 72 h at room temperature to be dried, and analysed with the same procedure. XRD patterns obtained for each tested varnish were compared against the reference patterns of hydroxyapatite (Reference code: 01-073-6113), NaF (00-036-1455), and TiO_2 (04-013-5313, 04-003-0844, and 04-003-0648).

2.6. Fourier Transform Infrared Spectroscopy (FTIR)

The FTIR (Spectrum GX, Perkin-Elmer, Waltham, MA, USA) analysis was performed on the liquid varnish samples prior to the immersion, and varnish powder after 48 h of Tris buffer immersion was tested using the FTIR. Data was collected from 1750 to 500 cm^{-1} wavenumbers. The FTIR analysis was also carried out on a pure NovaMin (Bioglass® 45S5) sample for reference purposes.

2.7. Magic Angle Spinning-Nuclear Magnetic Resonance Spectroscopy (MAS-NMR)

MAS-NMR was performed on the varnishes before and after immersion to investigate the chemical speciation of phosphorus and fluorine in the varnish. The integrated area under the NMR peak is proportional to the amount of the species present. In addition ^{19}F MAS-NMR unlike XRD enables fluorapatite to be distinguished from hydroxyapatite. The varnish samples before and after the immersion were analysed using the MAS-NMR spectroscopy (Bruker, Germany). Solid-state MAS-NMR experiments were carried out using the 600MHz Bruker spectrometer with the magnetic field of 14.1 Tesla. The ^{19}F and ^{31}P MAS-NMR spectra were collected at the resonance frequencies of 564.7MHz and 242.9MHz respectively. The sample was packed in 2.5mm o.d. zirconia rotor and spun at 20 kHz using the standard double resonance Bruker probe with low fluorine background. 1M aqueous solution of NaF producing a sharp signal -120ppm was used to reference ^{19}F chemical shift scale. 85% H_3PO_4 was used to reference the ^{31}P chemical shift scale. All experiments were run with 60 seconds recycle delay.

2.8. Statistical analysis

The differences in ion release at each time point and cumulatively among the test varnishes were statistically analysed using the repeated measurements of ANOVA and pairwise comparisons. Data analyses were performed using IBM SPSS Statistics 24.0 (SPSS Inc., Chicago, IL, USA). Sample size calculation was based on the data from a previous study [18]. The statistical power was set to 85% at a level of significance of 0.05 (two sided)

3. Results

3.1. Fluoride ion release

The initial fluoride release at 1 h of immersion was significantly higher for the CPP-ACPF varnish (0.593 mmol/g) compared to BGAF (0.187 mmol/g), and F (0.025 mmol/g) (p<0.001). However, F ion release was higher at 24 h immersion time point for both BGAF and F varnishes when compared to the CPP-ACPF varnish, with the values reaching 0.214 mmol/g (p<0.001), mmol/g, 0.0475, and 0.030 mmol/g respectively (Figure 2).

Cumulatively, the CPP-ACPF varnish showed the greatest fluoride ion release (1.113 mmol/g) when compared to both BGAF (0.638 mmol/g), and F alone (0.112mmol/g) varnishes across the 48 h immersion period (p≤0.001). However, there was a significant increase in the trend of ion release for the BGAF (p≤0.001), and slight increase for the F alone varnish at 6-48 h time interval when compared to the CPP-ACPF. Both CPP-ACPF and BGAF cumulative F ion release showed deviations from the square root time at later times compared with the F alone varnish (Figure 3). The expected total amount of fluoride ion in each varnish sample that was available to be released in 60 ml of Tris buffer was 1.775 mmol/g in all cases. There was a difference in the rate of fluoride release among the test varnishes, the CPP-ACPF exhibited the fastest fluoride release, followed by the BGAF and the F alone varnish gave the slowest release (Figure 4).

3.2. Calcium and phosphorus release

The highest initial burst of both calcium and phosphorus release was for the CPP-ACPF varnish, 0.0295 and 0.0516 mmol/g, compared to the BGAF varnish, 0.006 and 0.001 mmol/g respectively. The second burst in calcium ion release for both varnishes was at 6-24 h interval then a decreasing in release was observed for the remaining time period (Figure 5).

Over the 48 h, the CPP-ACPF varnish showed a significant increase in both calcium and phosphorus cumulative release in comparison to the BGAF varnish (p<0.001). Both varnishes showed more calcium ion

release after the 6 h time point immersion when compared to phosphorus release. Deviation of the cumulative calcium and phosphorus release from the square root time dependence at later times was identified for the CPP-ACPF varnish only (Figure 6).

Both CPP-ACPF and BGAF varnishes showed differences between the theoretical Ca:P ratio that would be expected for either CPP-ACP or NovaMin, and the measured Ca:P ratios in this study. The theoretical Ca:P ratio for ACP/CPP would be between 1.3 and 1.5 and the experimental values were lower than the minimum of 1.3. The theoretical Ca:P ratio for NovaMin should be about 5.2, whilst the Ca:P values of the BGAF started at 3.44 at 1h and increased to 4.56 at 48 h. (Figure 7).

3.3. X-Ray Diffraction (XRD)

The XRD pattern of each sample before immersion revealed several strong diffraction lines (filled black circles) at 38.7°, 56.0° and minor at 33.5° and 67.0° 2θ, all of which correspond to crystalline NaF (Figure 8). Another two minor diffraction lines at 29.0° and 35.0° were not identified. The XRD pattern of each sample after immersion failed to show significant diffraction lines for NaF and revealed the substantial presence of an amorphous phase with a broad diffraction halo at around 16° 2θ and second halo at around 22° 2θ. Two minor diffraction lines at 10.8° and 15.4° 2θ were present, however they were not identified.

The XRD patterns of BGAF varnish before and after immersion are illustrated in Figure 9. The pattern revealed diffraction lines at 38.8°, 56.1°, 33.5° and 67.0° 2θ confirming the presence of NaF in the sample before immersion. The lines became less pronounced after 48 hrs of immersion. Additional diffraction peaks at 25.4°, 37.9° and 48.1° 2θ corresponding to a titanium dioxide (anatase) a whitening agent were seen in the sample before immersion. TiO_2 remained after the immersion based on the diffraction line at 25.4° 2θ still being present (ii) in Figure 9. A small broad hump is seen around 30° 2θ in the sample before immersion was similar to the broad amorphous halo of the 45S5 glass powder (Figure S2 supporting information), which identified the presence of unreacted bioactive glass powder in the varnish sample. The original broad halo

disappeared after immersion in the test sample and a much broader and asymmetric hump appeared with the centre between 15° and 22° 2θ. A number of sharp, though relatively minor, diffraction lines can also be seen at 16.1°, 16.7° and 14.3° 2θ in addition to a small diffraction line at 10.8° 2θ in the pattern.

The XRD pattern of the fluoride alone varnish in Figure 10 before immersion showed the diffraction lines at 38.8°, 56.1°, 33.5° and 66.9° 2θ corresponding to NaF, NaF. Only two major diffraction lines 38.7° and 56.1° 2θ remained in the pattern of the sample after 48 hrs Tris immersion. The sample before immersion also showed the presence of titanium dioxide phase revealed by the presence of the diffraction lines at 25.3°, 37.7° and 48.1° 2θ. The sample after immersion showed a number of unidentified relatively strong diffraction lines at the positions of 16.0°, 16.7°, 14.3°, 8.4° and 10.8° 2θ. These diffraction lines were similar to those seen in the patterns of the immersed samples of two other varnishes (Figures 8&9) and therefore this might possibly be originating from partially crystallised hydrogenated rosin during immersion. It can also be seen that there was a broad amorphous halo pattern at around 16° 2θ in the immersed sample, which was quite close to the supressed broad intensity in the sample before immersion around the same 2θ values.

3.4. *Magic Angle Spinning-Nuclear Magnetic Resonance Spectroscopy (MAS-NMR)*

Figure 11 showed the ^{19}F MAS-NMR spectra of varnish samples before the immersion. The main signal seen in all spectra was relatively sharp line at about -225ppm. Thus, all the ^{19}F MAS-NMR spectra showed dominant presence of fluorine present as crystalline NaF. Since the dominance of the -225 pm signal was overwhelming, the spectra of the two samples with CPP-ACP and with bioactive glass were zoomed to reveal any other details in addition to the strong fluorine signal corresponding to NaF. From the spectra i and iii in Figure 11, there was a weak signal at between -104 and -105 ppm, which corresponded to a partially fluoride substituted apatite. The substitution by fluoride was partial and crystallinity of this apatite was low based on the position and linewidth of the signal.

Figure 12 shows the ^{19}F MAS-NMR spectra of the varnish samples collected after immersion. After 48 hrs Tris immersion, the ^{19}F MAS-NMR spectra of both BGAF (ii) and F alone (iii) varnishes showed the dominant presence of the fluorine-19 signal at around -225 ppm, which corresponded to the fluoride from the crystalline NaF. This signal was much less prominent in the spectrum of the CPP-ACPF varnish (i). All three spectra also contained a peak at around -109 ppm. This was close to the signal of fluoride in crystalline calcium fluoride CaF_2.

The ^{31}P MAS-NMR spectrum of the CPP-ACPF varnish (i, top spectrum in Figure 13) showed a single relatively broad peak at about 3 ppm. The BGAF varnish before immersion presented a broad feature at 8.4 ppm, and small sharp signal at about 2.2 ppm (ii, bottom spectrum in Figure 13).

The ^{31}P MAS-NMR spectra of the CPP-ACPF and BGAF varnishes failed to show a signal following the immersion as seen in Figure 14. This meant no phosphorus species were left in these varnishes after the immersion.

4. Discussion

It is worth noting that all three varnishes had the same total NaF content (5%). Thus, the different kinetics of release are probably due to the additional component (CPP-ACP/bioactive glass) and/or the different resins used. The maximum ion release was for the CPP-ACPF followed by BGAF, and F varnish had the lowest release. Both calcium phosphate based varnishes are a source of bioavailable fluoride, calcium and phosphate ion. Tris buffer was used in the current study as an immersion solution to investigate the ion release behaviour, rather than the simulated body fluid or artificial saliva that would more closely mimic the natural saliva. This was to exclude the effect of the additional calcium and phosphate from these fluids, which may camouflage the potential ion release from the test materials [28], [29]. The immersion solution was changed at each time point to simulate the effect of saliva exchange as *in vivo* condition and ion measurement was performed. Studying ion release with a longer time of immersion, more than 48 h, wasn't considered in

this study, due to the fact these dental varnishes would be unlikely to be retained on tooth surface for much longer than this time period due to the potential removal during mastication and by salivary fluids. It was reported that retention of dental varnishes are limited in the oral cavity for only several hours following application [1].

In this study, a uniform film thickness of varnish was achieved by applying an equal amount of varnish spread over a standardised area to minimise sample to sample variations that would influence the ion release. In addition, the samples were promptly applied to the substrate to reduce the possible change in varnish weight as a result of evaporating the volatile constituents such as isopropanol and ethanol that might affect ion load percentage in each sample.

4.1. Fluoride

The highest initial burst of fluoride together with the maximum total amount of fluoride released over 48 h was for the CPP-ACPF varnish, could be related to the differences in their chemical composition, and physical properties, including resin type, density, viscosity, and particles size [30], [31], [32]. Water sorption and solubility of dental materials have a significant impact on their performance, since water could encourage a range of chemical and physical processes that influence the structure and function of the material itself [33]. It was reported that dissolution time of polyvinyl acetate (PVA) as a water soluble polymer was relatively short [34], and the maximum burst was in the first hour of immersion [35], which was consistent with the trend of fluoride ion release from the CPP-ACPF varnish. PVA has a higher ability to blend due to its polarity and CO2 affinity amongst other proposed polar structures. The interaction between the residual carbonyl groups on the polar gases, such as CO2, and the morphological changes possibly would increase solubility [36], [37]. In this respect, the PVA solubility is substantially increased in the presence of organic solvents [38]. Therefore, it can be suggested that the presence of PVA in addition to ethanol within the CPP-ACPF varnish formulation may contribute to a higher dissolution rate and faster ion release compared to other varnishes tested. This result was also consistent with a previous finding that a combination of polyethylene co-vinyl acetate and NaF resulted in a higher initial burst effect and short release time compared with a same formula

of varnish plus an additional polyethylene co-vinyl acetate coat [39]. In addition, the presence of ethanol in the CPP-ACPF formula might easily evaporate leaving pores that are likely to facilitate water movement through the varnish [40]. In contrast, the presence of isopropanol in both BGAF and F varnishes, this is less likely to evaporate compared to the ethanol [41]. In a recent study, it was reported that the CPP-ACPF varnish has small and homogenous particles, facilitating ion release compared with both BGAF and F varnishes that have large particles (unpublished data, Operative Dentistry) (Figure S1). These authors suggested that the large particles may take longer to dissolve in the immersion solution.

The lowest initial burst and cumulative fluoride ion release for both BGAF and F varnishes might also be related to the presence of Urethane methacrylate resin in their compositions. This resin is less soluble and has a lower water sorption, [42], [43], which would be expected to result in less ion release and this was observed throughout this study. Therefore, both these varnishes are less likely to take up water to swell, dissolve and subsequently to release ions, which could explain the retained substantial amount of fluoride ions retained particularly for the varnish containing fluoride alone. In addition, the burst release was lower for the BGAF and undetected for the F varnish when compared to the CPP-ACPF formula with the PVA resin.

The other possible cause for this variation in fluoride release between the test varnishes could be related to the high solubility of CPP-ACP complex in aqueous solution [44], which might enhance the dissolution of NaF particles in the immersion buffer. This was supported by previous findings where the CPP-ACPF provided the highest fluoride ion release compared to different calcium phosphate formulations and fluoride alone varnishes [18], [19]. Mehta (2014) [45] reported that CPP-ACP was unlikely to adhere to the tooth surface due to its amorphous nature when compared to the firmly attached bioactive glass particles [38], [42], [43].

The BGAF had a higher fluoride release compared to the varnish fluoride alone. This could be due to the ability of BGA to release calcium, sodium, and phosphate in an aqueous solution. This permits for an ionic exchange of Na^+ for H^+ or H_3O^+ at the glass-liquid interface, allowing the formation of saturated ionic reservoir in the immersion solution [22]. This potentially allows the varnish to dissolve following the Tris immersion by

releasing more fluoride compared to the F alone varnish. However, both BGAF and F varnishes, excluding the initial burst at 1 h time point, showed the same burst of F release that started at 6 h time point and the maximum release was at 24 h. This could be due to both varnishes having the same additives, including the type and the percentage of the carrier resin. The existence of urethane methacrylate in both varnishes that is unlikely to swell, again would delay the burst effect compared to the PVA effect in the CPP-ACP formulation. However, it should be noted that the period of immersion in Tris buffer for the 24 h time point was 18 h compared to the smaller time increments before this that probably led to seemingly high concentration measured at 24 h. This apparent artefact was not present in the cumulative release plots.

The cumulative ion release were plotted in a square root time dependence at early times and indicates a linear relationship indicative of a diffusion controlled mechanism. However, at later times they may deviate from linearity. At longer times, the fluoride release for the CPP-ACPF varnish no longer exhibited a square root time dependence. This was possibly due to the release of most of the fluoride. The BGAF varnish also exhibited this effect, however it occurred at longer times due to the slower fluoride release. This effect was not observed for the F varnish, which exhibited a square root time dependence till the longest time point studied (Figure 3).

Interestingly, the results from the XRD supported the findings of ion release. The amount of NaF crystals at the baseline before the immersion was high in all varnishes. Whilst after 48 h immersion there was no NaF left in the CPP-ACPF and seemed to be unclearly detected in CPP-ACPF, identified in BGAF, and more apparent in the F alone varnish after 48 h immersion.

The ^{19}F MAS-NMR spectra of the varnish powders confirmed the dominant nature of fluorine in all cases before the immersion (Figure 11). The detection of fluorapatite crystals even in small amounts in the samples powder of CPP-ACP and BAGF before immersion may be due to; i) the reaction of varnish ingredients within the varnish container, or ii) it could be due to reaction and crystallization during the extraction process during powder preparation. The amount of fluorapatite detected in the CPP-ACP powder is much smaller than with

the BGAF powder. The presence of the peptide αS1-CN (59–79) in the CPP-ACP structure might potentially aid in stabilising fluoride, calcium and phosphate in an aqueous solution in the pH range of 6-9 thereby preventing calcium phosphate and fluoride ions forming fluorapatite [16], [17].

With time, the amount of NaF reduced in the varnishes. This was most marked for the CPP-ACPF that released the most fluoride whilst XRD detected no crystalline NaF a very small amount is present in the 19F spectrum with a chemical shift at -225ppm. In addition there is a small amount of CaF2 present with a chemical shift at -108ppm within the varnish. There was no evidence of fluorapatite forming that would exhibit a peak at -103ppm. This was supported by the absence of a peak for apatite in the ^{31}P spectra after immersion. The BGAF had a similar behaviour, however there was much more NaF left in the varnish at 48 h. There was again no evidence of any fluorapatite forming in the varnish. This was also supported by the absence of a signal for apatite at about 3ppm in the ^{31}P spectra. The F alone varnish exhibited the strongest NaF signal at 48 h. Neither CaF_2 nor fluorapatite could be formed due to the lack of calcium and phosphate. This varnish released the least cumulative amount of fluoride at 48 h, which is in agreement with the large amounts found after immersion by NMR and XRD.

The detection of CaF_2 in the CPP-ACPF reported in this paper following the immersion, however not before the immersion, could be due to the presence of the active sequence –Ser(P)-Ser(P)-Ser(P)-Glu-Glu- in the CPP-ACP formulation that has a remarkable effect in stabilising calcium and phosphate as nanoclusters of ions in metastable solution [46]. This allows the CPP to bind to forming nanoclusters of calcium and phosphate ions to form nanocomplexes of approximately 1.5 nm radius, inhibiting their growth to the critical size required for nucleation and phase transformation [47]. This complex is highly soluble in water releasing their ions that can combine with fluoride to form CaF_2. Similarly, the BGA can commence the ion exchange following the contact with an aqueous solution [Hench 1998]. The CaF_2 is very insoluble [48]. Thus, this compound can be precipitated or formed on the varnish surface following the immersion, and detected by the NMR spectra.

Based on the nominal content of fluoride and the expected total amount of fluoride that should be released from each varnish sample in 60 ml of Tris buffer (1.775 mmol/g), the CPP-ACPF approximately released more than 62.7% of the total amount of F in sample varnish, BGAF 35.9%, and F 6.3%. Accordingly, CPP-ACPF varnish released most of its fluoride content following the immersion, whilst both BGAF and F varnishes retained more fluoride ions and clearly the release possibly would therefore be longer for these two varnishes. Nevertheless, the percent of ion release would not completely reflect the actual released amount as both F-ISE can detect the free ion only and is not capable of detecting fluoride in the CaF_2 and fluorapatite crystals.

4.2. Calcium and phosphorus

The initial burst of calcium and phosphorus release was higher for the CPP-ACPF, when compared to the BGAF. It can also be speculated that this variation could be related to their chemical compositions and physical properties [30], [31], [32]. The total amount of both calcium and phosphorus released from the CPP-ACPF was higher than the BGAF varnish. This was probably due to the amount of calcium and phosphorus being much higher in the CPP-ACP complex compared to the BGA. Calcium and phosphorus are the major constituents of the CPP-ACP whilst the BGA 45S5 is composed of 46.1 SiO_2, 2.6 P_2O_5, 24.4 Na_2O and 26.9 CaO (mol%) [49]. In both varnishes, the amount of calcium released was higher than the amount of phosphorus. This might also be related to the variation in Ca:P ratio in their compositions approximately 3:2 and 10:1 for the CPP-ACP and BGA respectively [17], [49]. The difference in Ca:P ratio was clearly seen in 24 h time point of both CPP-ACP and bioglass varnishes, where the maximum release of calcium in both varnishes was much greater than P (Figure 5).

The high calcium ion release from the CPP-ACPF was also revealed in previous studies compared to fluoride varnishes, either with modified tricalcium phosphate (Clinpro White, 3M ESPE, MN, USA), dibasic sodium phosphate and calcium sulfate dihydrate (Enamel Pro, Premier Dental Products, PA, USA), calcium fluoride (Bifluorid 5 Voco, Cuxhaven, Germany), or fluoride alone (Duraphat Colgate Oral Care, NSW, Australia) [18]. The bioavailability of calcium and phosphate ions in the CPP-ACP formula in addition to the high solubility of the complex in water might be a reason for the differences in quantity and time of calcium release [18], [44].

The difference between the theoretical ratio and the experimental ratio for both the CPP-ACPF and BGAF that was shown in this study (Figure 7) could be due to the formation of CaF_2 that was seen to form in the ^{19}F Spectra (Figure 12). The formation of CaF_2 would consume calcium and reduce the Ca:P ratio.

The general trend of calcium and phosphorus release of the BGAF varnish was almost comparable to the F release and reflecting the ability of this varnish to release ions not only for the first 6 h time point immersion but also for the following hours compared to the CPP-ACPF which released most of its ions earlier at the 1-6 h time point. This could again be related to the type of carrier used in the varnish, Urethane dimethacrylate that will not dissolve by water [42], [43]. However, the CPP-ACPF varnish showed an increase in calcium release at 6 h immersion following the dramatic decrease in the first 6 h which was inconsistent with the continuous decrease in fluoride release. This could be related to the consumption of a significant fraction of the calcium ions by the formation of CaF_2 in the first 6 h, whilst after 6 h time point, the amount of fluoride was insufficient to consume total amount of free calcium ion. Therefore, this explains the dramatic increase in calcium ion concentration in the immersion solution. The difference in the quantity of calcium/phosphorus released at 24 h was also noticed in the BGAF varnish. This could again be the long immersion period, time point 6 to 24 h, that would consume most of the released fluoride to form CaF_2 leaving the calcium ion free in the immersion solution that can be detected by ICP-OES. The variation in Ca:P ratio in the structure of both CPP-ACP and BGA would be another reason for this difference. In addition, the longer immersion time between 6 h and 24 h time points might cause such increase in calcium ions at 24 h point as discussed for the fluoride data at 24 h immersion time point.

The ^{31}P MAS-NMR confirmed the presence of phosphorus in both CPP-ACPF and BGAF varnishes before immersion, however it was not present after 48 h, this implies all the phosphorus was released.

The FTIR spectra supported that the type of BGA in the BGAF varnish was 45S5 (Figure S2). There was no sign of apatite formation detected after 48h h Tris immersion in the test varnishes (Figure S3-S5). This was consistent with the NMR results.

5. Conclusion

This laboratory based study provided evidence that thec study CPP-ACPF and BAGF varnishes provide fluoride bioavailability in addition to calcium and phosphate. The dental varnish containing CPP-ACP and fluoride, released more ions (Ca, P and F) when compared to the bioactive glass varnish, whilst the fluoride alone varnish appeared to retain fluoride longer over the study period. The variation in chemical compositions of inactive ingredients and/or calcium phosphate system influences the dynamics of ion release, regardless of fluoride content. This is of clinical value regardless of the releasing time (short/long) and could potentially enhance the remineralisation process, both on enamel and dentine.

References

1. Beltrán-Aguilar ED, Goldstein JW, Lockwood SA. Fluoride varnishes. A review of their clinical use, cariostatic mechanism, efficacy and safety. J Am Dent Assoc, 2000;131:589-596.
2. Azarpazhooh A and Main PA. Fluoride varnish in the prevention of dental caries in children and adolescents: a systematic review. J Can Dent Assoc, 2008;74:73–9.
3. Ekstrand K, Martignon S and Holm-Pedersen P. Development and evaluation of two root caries controlling programmes for home-based frail people older than 75 years. Gerodontology, 2008;25:67-75.
4. Gibson G, Jurasic MM, Wehler CJ and Jones JA. Supplemental fluoride use for moderate and high caries risk adults: a systematic review. J Public Health Dent, 2011;71:171–84.
5. Karabekiroglu S. S and ˘ Unl¨u N. Effectiveness of different preventive programs in cariogram parameters of young adults at high caries risk. Int J Dent, 2017;7189270:1-10.
6. Rossa Al, Sherriff A,Kidd J, Gnich W, Anderson J, Deas L and Macpherson L. A systems approach using the functional resonance analysis method to support fluoride varnish application for children attending general dental practice. Appl Ergon, 2018;68:294–303.
7. Papas A, Russell D, Singh M, Stack K, Kent R, Triol C et al. Double Blind Clinical Trial of a Remineralizing Dentifrice in the Prevention of Caries in a Radiation Therapy Population. Gerodontology, 1999;16:2-10.

8. Reynolds E. Calcium phosphate-based remineralization systems: Scientific evidence? Aust Dent J, 2008;53:268-273.
9. Ten Cate J.M and Featherstone J.D.B. Mechanistic aspects of the interactions between fluoride and dental enamel. CRC Crit Rev Oral Biol Med, 1991;2:283-296.
10. Ten Cate J.M. Review on fluoride, with special emphasis on calcium fluoride mechanisms in caries prevention. Eur J Oral Sci, 1997;105:461-465.
11. Hay KD and Thomson WM. A clinical trial of the anticaries efficacy of casein derivatives complexed with calcium phosphate in patients with salivary gland dysfunction. Oral Surg Oral Med Oral Pathol Oral Radiol Endod, 2002;93:271–275.
12. Dawes C. Physiological Factors Affecting Salivary Flow Rate, Oral Sugar Clearance, and the Sensation of Dry Mouth in Man. Journal of Dental Research, 1987; 66(2 suppl):648-653.
13. Vogel G.L. Oral fluoride reservoirs and the prevention of dental caries. M.A.R. Buzalaf (Ed.), Fluoride and the Oral Environment. Monogr Oral Sci. Basel, Karger, 2011;22:146–157.
14. Ericsson Y. Fluorides in dentifrices. Investigations using radioactive fluorine. Acta Odontol Scand, 1961;19:41–77.
15. Benzian H, Holmgren C, Buijs M, van Loveren C, van der Weijden F and van Palenstein Helderman W. Total and free available fluoride in toothpastes in Brunei, Cambodia, Laos, the Netherlands and Suriname. Int Dent J, 2012; 62:213-221.
16. Reynolds EC, Black CL, Cai F, Cross KJ, Eakins D, Huq NL, et al. Advances in enamel remineralization: casein phosphopeptide-amorphous calcium phosphate. J Clin Dent, 1999; 2:86-88.
17. Cross KJ, Huq NL, Stanton DP, Sum M and Reynolds EC. NMR studies of a novel calcium, phosphate and fluoride delivery vehicle-α(S1)-casein(59–79) by stabilized amorphous calcium fluoride phosphate nanocomplexes. Biomaterials, 2004;25:5061-5069.
18. Cochrane NJ, Shen P and Yuan Y, Reynolds EC. Ion release from calcium and fluoride containing dental varnishes. Aust Dent J, 2014;59:100–105.
19. Shen P, Bagheri R, Walker GD, Yuan Y, Stanton DP, Reynolds C, et al. Effect of calcium phosphate addition to fluoride containing dental varnishes on enamel demineralization. Aust Dent J, 2016;61:357-365.

20. Tao S, Zhu Y, Yuan H, Tao S, Cheng Y, Li J and He- PloS one L. Efficacy of fluorides and CPP-ACP vs fluorides monotherapy on early caries lesions: A systematic review and meta-analysis. Journals.plos.org, 2018, PLoS ONE 13(4): e0196660. https://doi.org/10.1371/journal.pone.0196660
21. Gjorgievska ES and Nicholson JW. A preliminary study of enamel remineralization by dentifrices based on Recalden (CPP-ACP) and Novamin (calcium-sodium-phosphosilicate). Acta Odontol Latinoam, 2010;23:234–9.
22. Hench LL. Bioceramics: From Concept to Clinic. J Am Ceramic Soc, 1991; 74(7):1487–1510.
23. El-Wassefy N.A. Remineralizing effect of cold plasma and/or bioglass on demineralized enamel. Dent. Mater, 2017;36:157–167.
24. Fernando D, Attik N, Pradelle-Plasse N, Jackson P, Grosgogeat B and Colon P. Bioactive glass for dentin remineralization: A systematic review. Mat Sci Eng C, 2017; (76):1369-1377.
25. Taha A.A, Patel M.P, Hill R.G and Fleming P.S. The effect of bioactive glasses on enamel remineralization: a systematic review. J Dent, 2017;67:9-17.
26. Sleibi A, Tappuni AR, Davis GR, Anderson P and Baysan A. Comparison of efficacy of dental varnish containing fluoride either with CPP-ACP or bioglass on root caries: *Ex vivo* study. J Dent, 2018;73:91-96.
27. Mneimne M, Hill RG, Bushby AJ and Brauer DS. High phosphate content significantly increases apatite formation of fluoride-containing bioactive glasses. Acta BIiomater, 2011; 7:1827-1834.
28. Fagerlund S, Hupa L and Hupa M. Dissolution patterns of biocompatible glasses in 2-amino-2-hydroxymethyl-propane-1,3-diol (Tris) buffer. Acta Biomater, 2013;9:5400-5410.
29. Kirste G, Brandt-Slowik J, Bocker C, Steinert M, Geiss R and Brauer DS. Effect of chloride ions in Tris buffer solution on bioactive glass apatite mineralization. Int J Appl Glass Sci, 2017;8:438 –449.
30. Castilllo JL, Milgron P, Kharasch E, Izutsu K and Fey M. Evaluation of the fluoride release from commercially available fluoride varnishes. J Am Dent Assoc, 2001;132:1389–1392.
31. Shen C and Autio-Gold JT. Assessing fluoride concentration uniformity and fluoride release from three varnishes. J Am Dent Assoc, 2002;133:176–182.

32. LaTorre G and Greenspan DC. The role of ionic release from NovaMin (calcium sodium phosphosilicate) in tubule occlusion: an exploratory *in vitro* study using radio-labeled isotopes. J Clin Dent, 2010;21:72-6.
33. Park J, Ye Q, Topp E, Misra A, Kieweg S.L and Spencer P. Water sorption and dynamic mechanical properties of dentin adhesives with a urethane-based multifunctional methacrylate monomer. Dent Mater, 2009;25:1569-1575.
34. Kolter K, Wichtner M, Schönherr M and Mittwollen J. Pharmaceutical formulation for producing rapidly disintegrating tablets. US Patent, 2013; abstract no. US8425935B2. https://patents.google.com/patent/US8425935B2/en.
35. Morita R, Honda R and Takahashi Y. Development of oral controlled release preparations, a PVA swelling controlled release system (SCRS). I. Design of SCRS and its release controlling factor. J Control Release, 2000;63:297-304.
36. Leijtens T , Ding I.K, Giovenzana T, Bloking J.T, McGehee M.D and Sellinger A. Hole transport materials with low glass transition temperatures and high solubility for application in solid-state dye-sensitized solar cells. ACS Nano, 2012;6:1455-1462.
37. Chen C.L, Teng H and Lee Y.L. Preparation of highly efficient gel-state dye-sensitized solar cells using polymer gel electrolytes based on poly (acrylonitrile-co-vinyl acetate). J. Mater. Chem, 2010;21:628− 632.
38. Wang L, Zhang H, Wang C and Ma T. Highly stable gel-state dye-sensitized solar cells based on high soluble polyvinyl acetate ACS Sustain. Chem. Eng; 2013;1:205-208.
39. Baturina O, Tufekci E, Guney-Altay O, Khan SM, Wnek GE and Lindauer SJ. Development of a sustained fluoride delivery system. Angle Orthod, 2010;80:1129-1135.
40. Earl M.S.A, Mount G.J and Hume G.R. The effect of varnishes and other surface treatments on water movement across the glass ionomer cement surface. Aust Dent J, 1989;34:326-329.
41. Mülhardt C. Der Experimentator: Molekularbiologie/Genomics. Spektrum Akademischer Verlag Heidelberg. 2009; ISBN 978-3-8274-2036-7 page 38.
42. Delbem A.C.B, Brighenti F.L, Oliveira F.A.L, Pessan J.P, Buzalaf M.A.R and K.T. Sassaki. In vitro assessment of an experimental coat applied over fluoride varnishes. J Appl Oral Sci, 2009;17:280-283.

43. Ortengren U, Wellendorf H, Karlsson S and Ruyter I.E. Water sorption and solubility of dental composites and identification of monomers released in an aqueous environment. J Oral Rehabil, 2001;28:1106-1115.
44. Cochrane NJ and Reynolds EC. Casein phosphopeptides in oralhealth. In: Wilson M, ed. Food constituents and oral health: current status and future prospects. Cambridge: Woodhead Publishing Limited, 2009.
45. Mehta AB, Veena Kumari RJ and Izadikhah V. Remineralization potential of bioactive glass and casein phosphopeptide-amorphous calcium phosphate on initial carious lesion: An in-vitro ph-cycling study. J Conserv Dent, 2014;17:3-7.
46. Cochrane NJ, Saranathan S, Cai F, Cross KJ and Reynolds EC. Enamel subsurface lesion remineralisation with casein phosphopeptide stabilised solutions of calcium, phosphate and fluoride. Caries Res, 2008;42:88–97.
47. Reynolds EC. Casein phosphopeptide-amorphous calcium phosphate: the scientific evidence. Adv Dent Res, 2009;21:25–29.
48. Øgaard B. CaF2 formation: Cariostatic properties and factors of enhancing the effect. Caries Res, 2001;35(suppl 1):40-44.
49. Hill R.G and Brauer D.S. Predicting the bioactivity of glasses using the network connectivity or split network models. J Non-Cryst Solids, 2011;357:3884-3887.

Figure

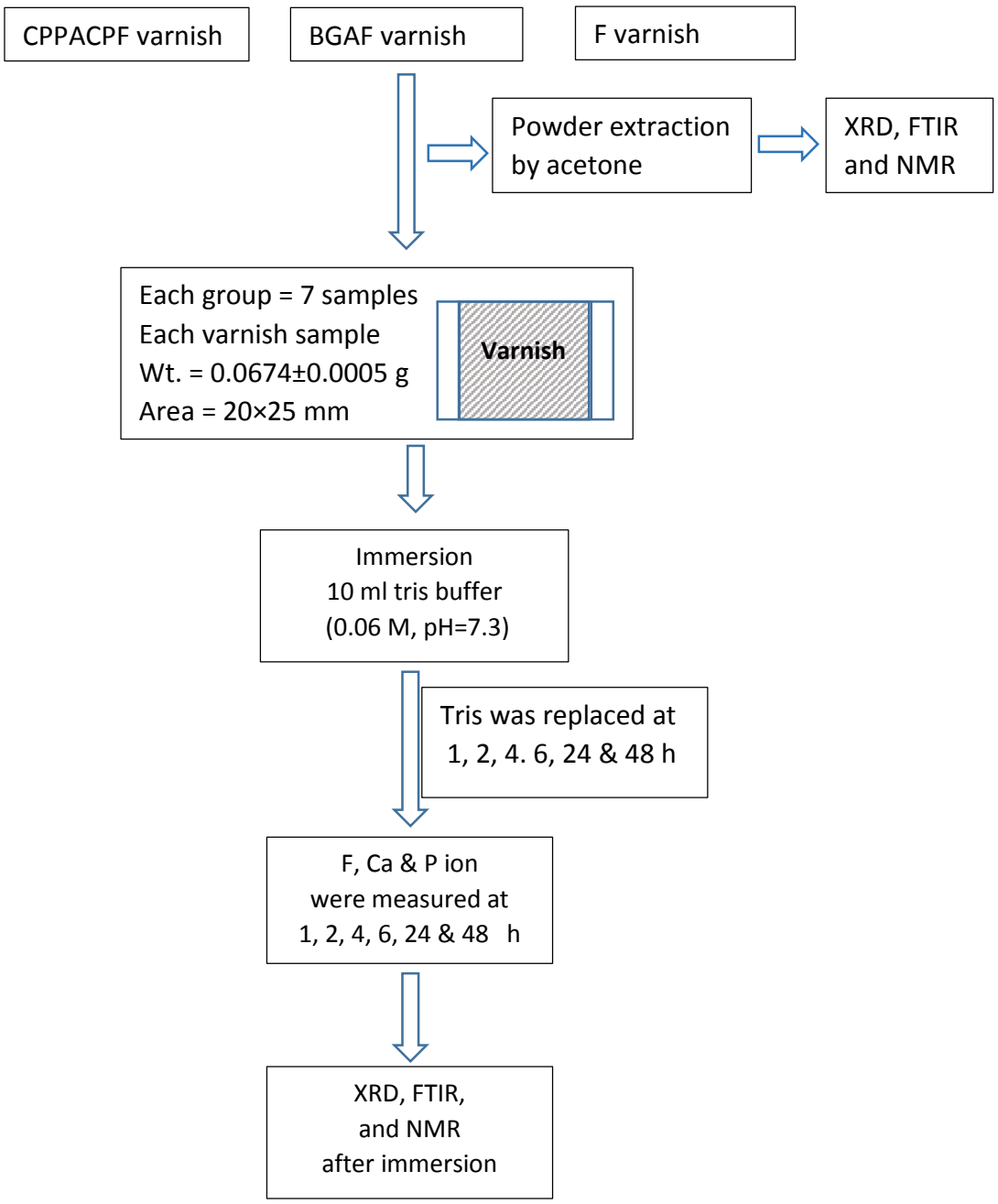

Figure 1. Study flow chart.

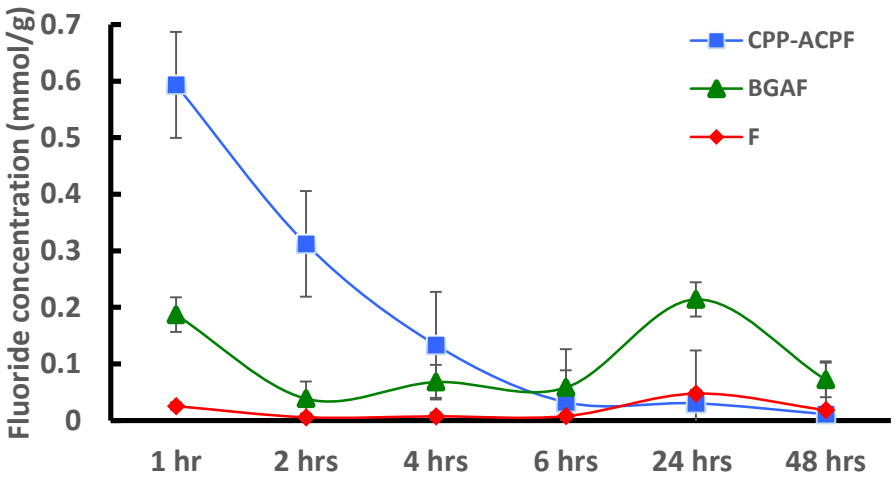

Figure 2. Non-cumulative F ion release at each time point in tris buffer (mmol/g).

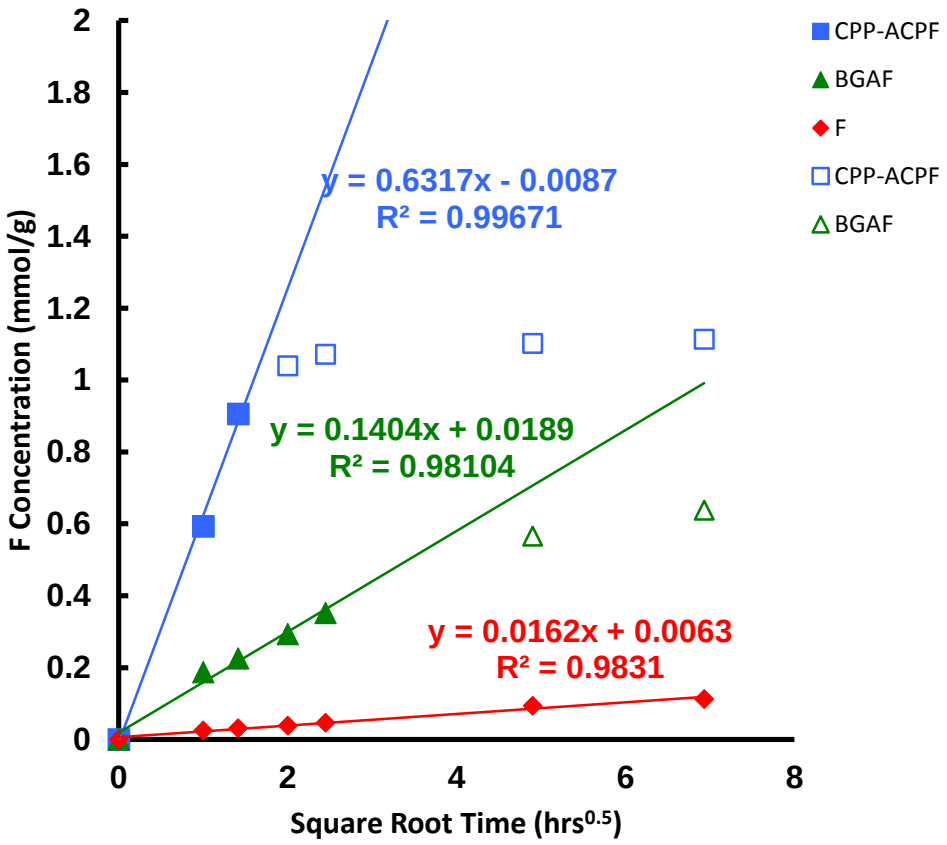

Figure 3. Cumulative F ion release of each varnish in the tris buffer (mmol/g)using square root time on x –axis dependence at early times (lines). The empty shapes represent the actual values of fluoride ion release.

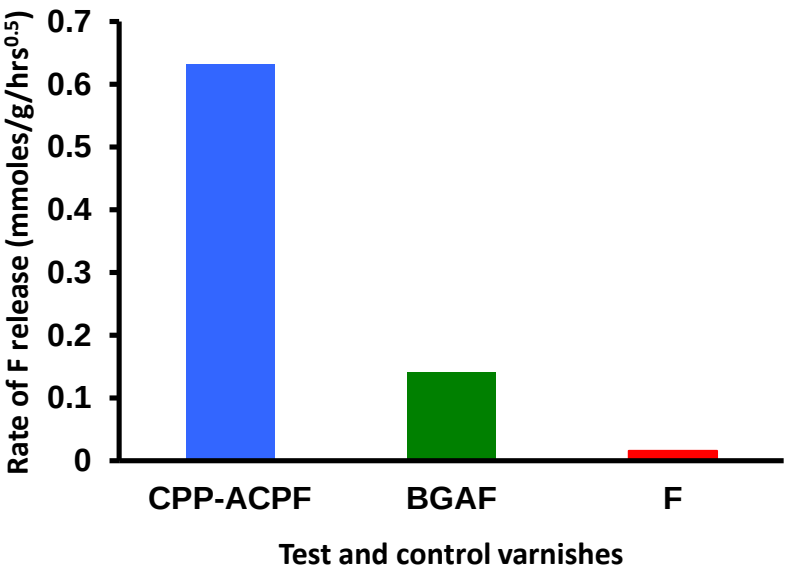

Figure 4. Rate of fluoride ion release of each varnish in the tris buffer over 48 h.

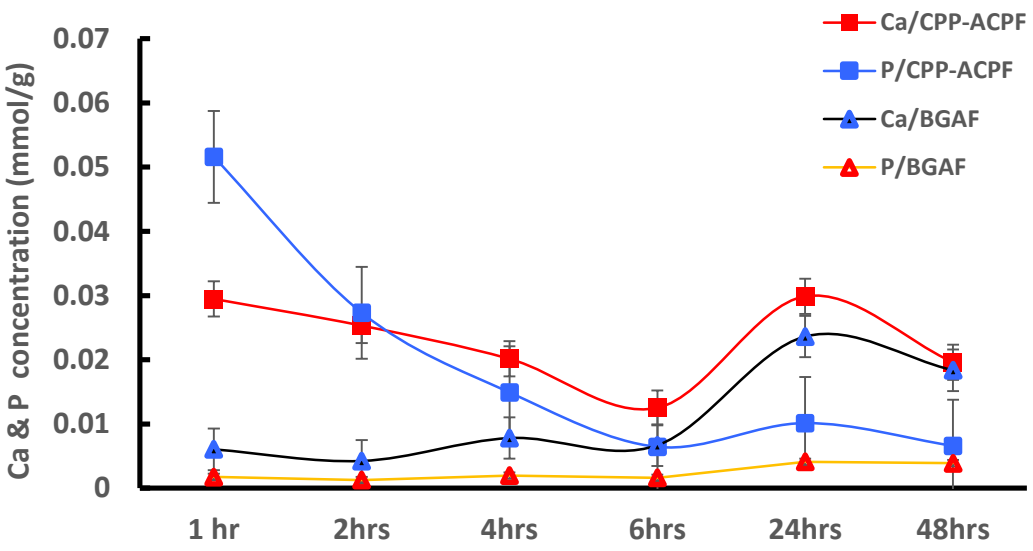

Figure 5. Non-cumulative calcium (Ca) and phosphate (P) ion release for the CPP-ACPF, and BGAF varnishes in tris buffer (mmol/g).

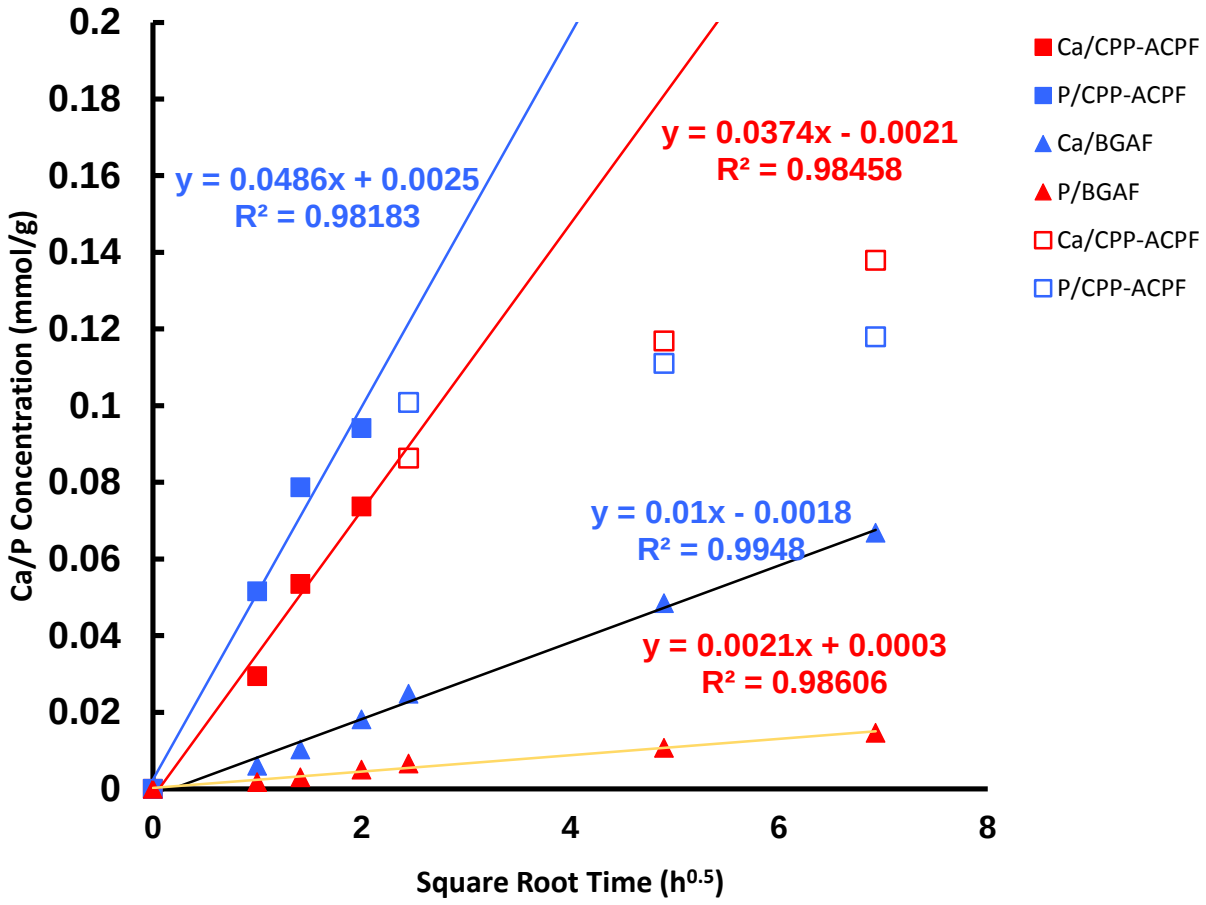

Figure 6. Cumulative calcium (Ca) and phosphate (P) ion release over 48 h for the CPP-ACPF, and BGAF varnishes in tris buffer (mmol/g) using square root time on x –axis. The empty shapes represent the actual values of ion release.

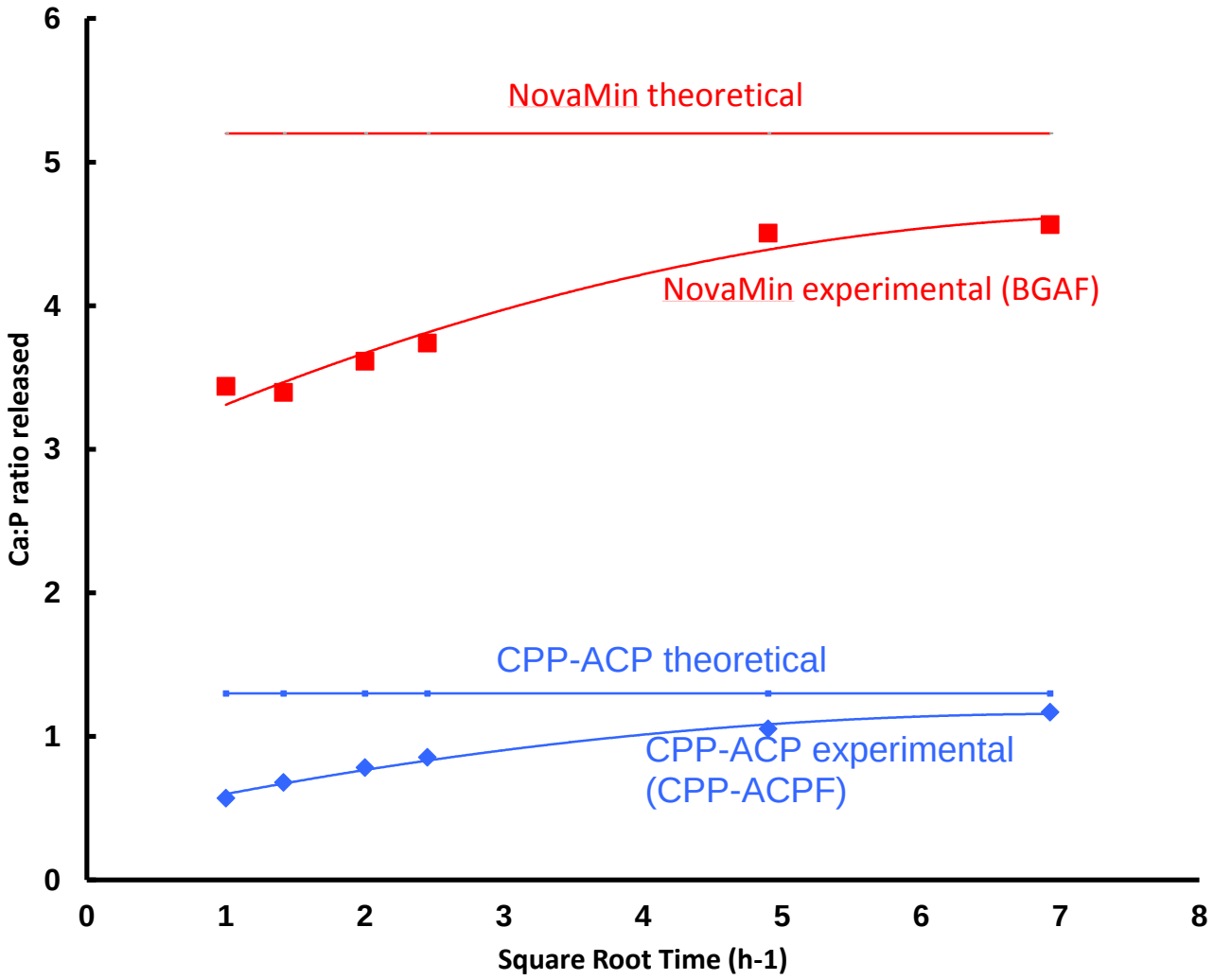

Figure 7. Difference between the theoretical and measured Ca:P ratio for both the CPP-ACPF and BGAF.

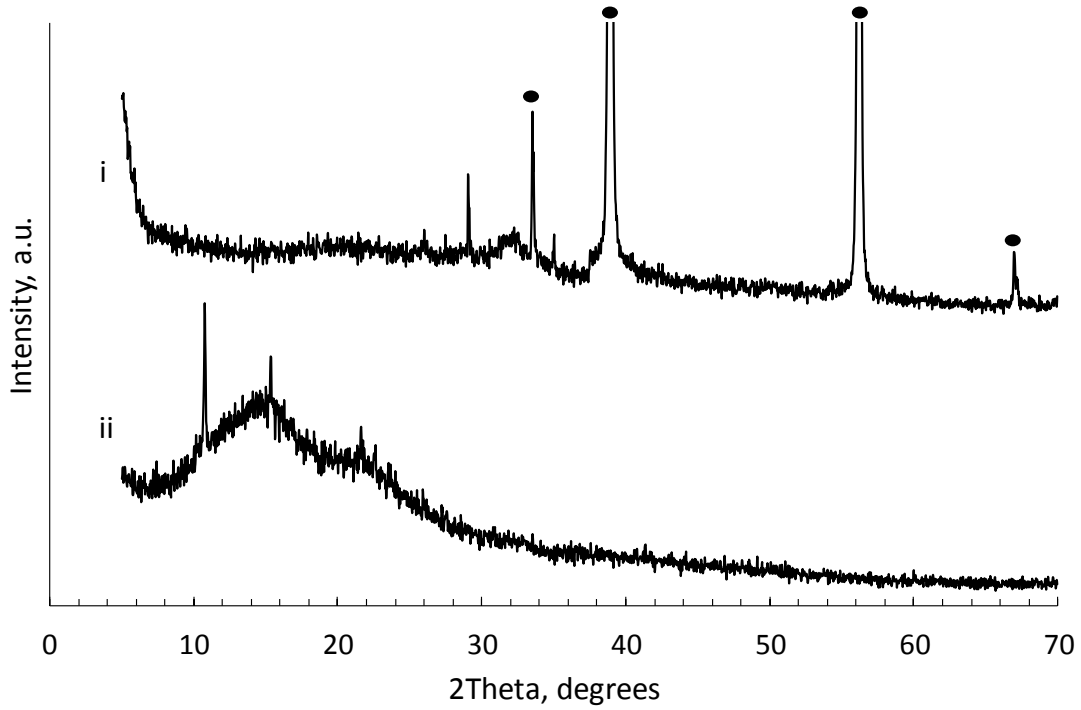

Figure 8. XRD pattern of CPP-ACPF varnish before (i) and after 48 h immersion in tris buffer (ii).

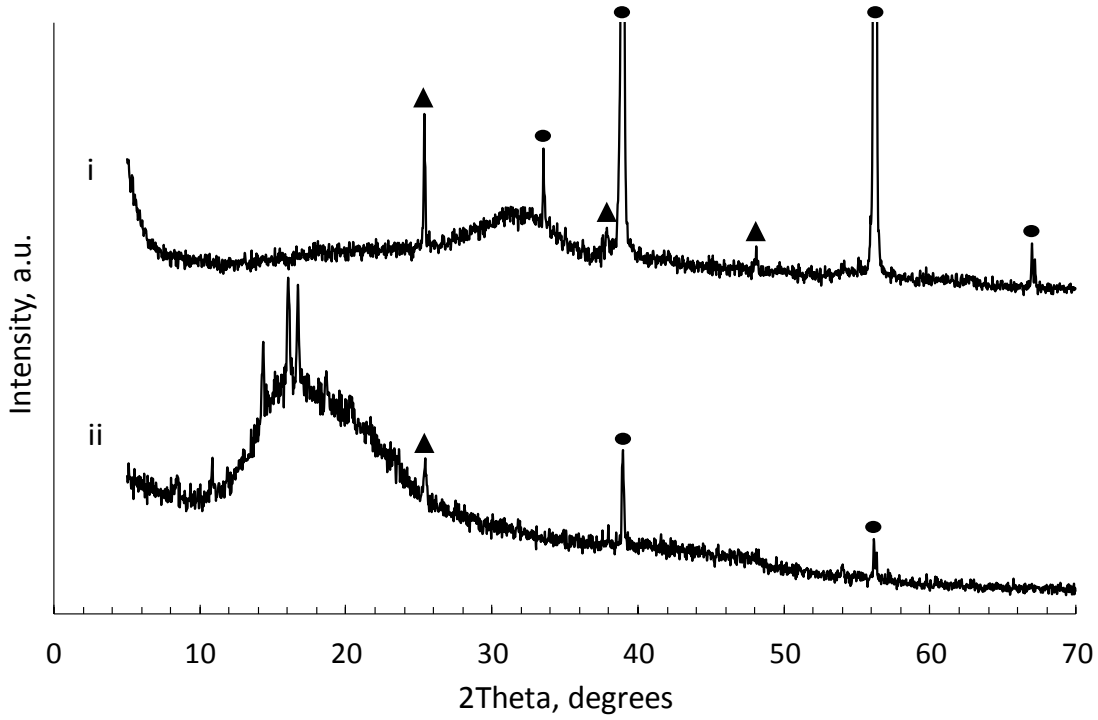

Figure 9. XRD pattern of BGAF varnish before (i) and after 48 hrs tris immersion (ii).

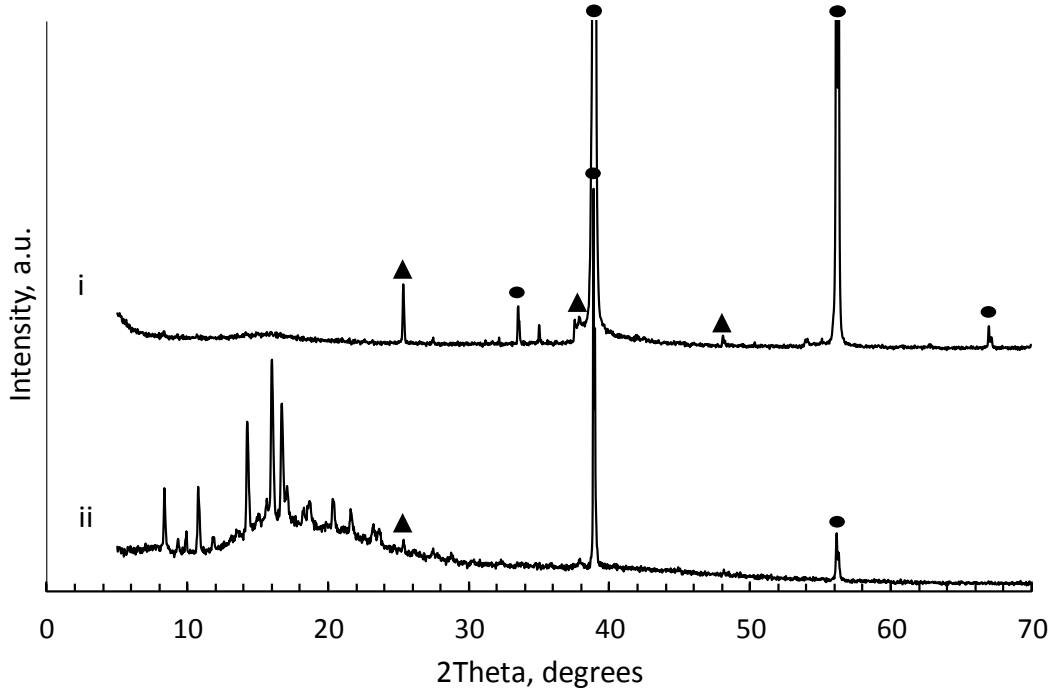

Figure 10. XRD pattern of F alone varnish before (i) and after 48 hrs tris immersion (ii).

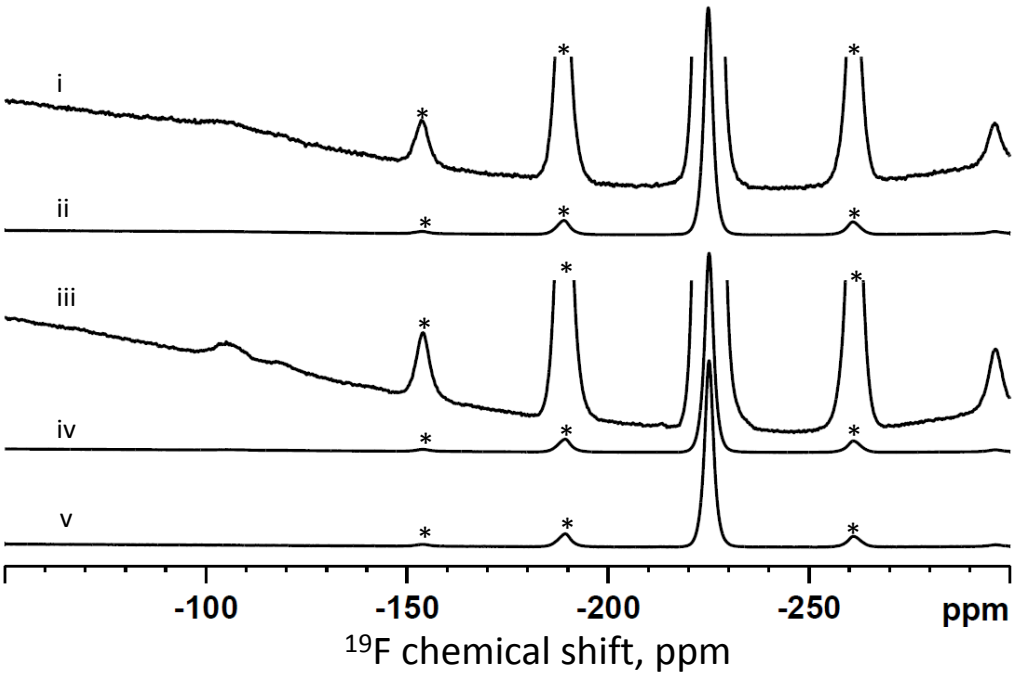

Figure 11. ^{19}F MAS-NMR spectra of the test varnishes (powders extracted by acetone) before immersion; i, ii – CPP-ACPF, iii, iv – BGAF, v – F. Asterisks show spinning side bands.

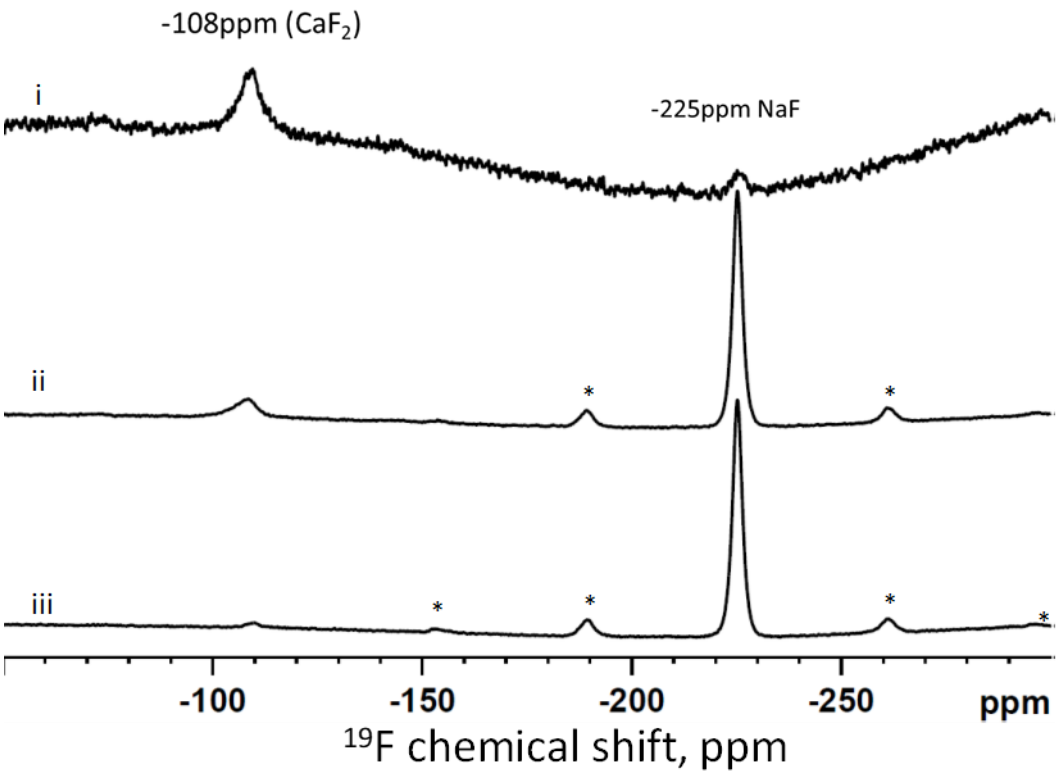

Figure 12. ^{19}F MAS-NMR spectra of the test varnishes following 48 hrs immersion in tris buffer: i - CPP-ACPF; ii – BGAF; iii – F.

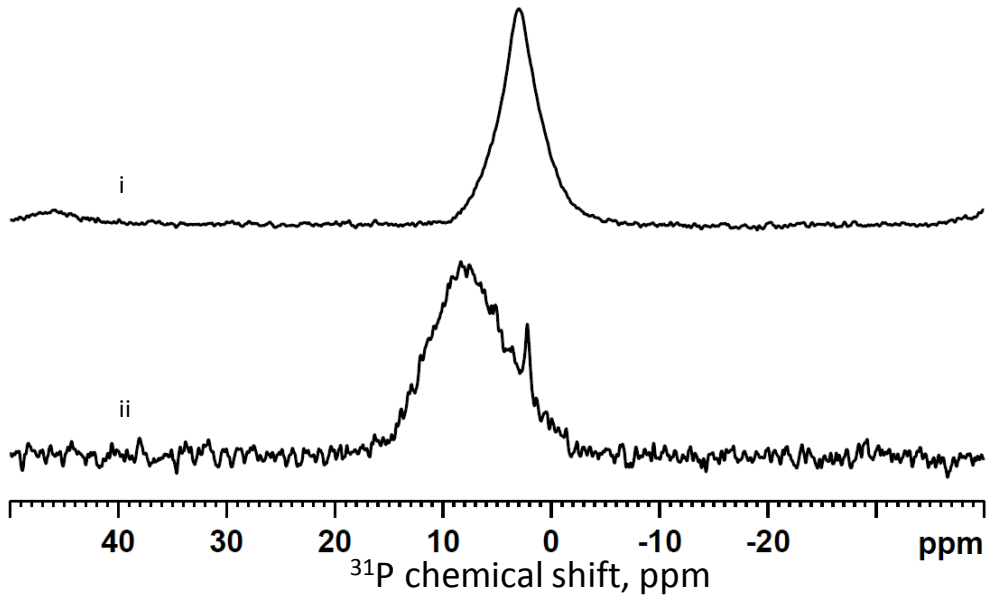

Figure 13. ^{31}P MAS-NMR spectrum of the CPP-ACPF (i) and BGAF (ii) varnishes (powders extracted by acetone) before immersion.

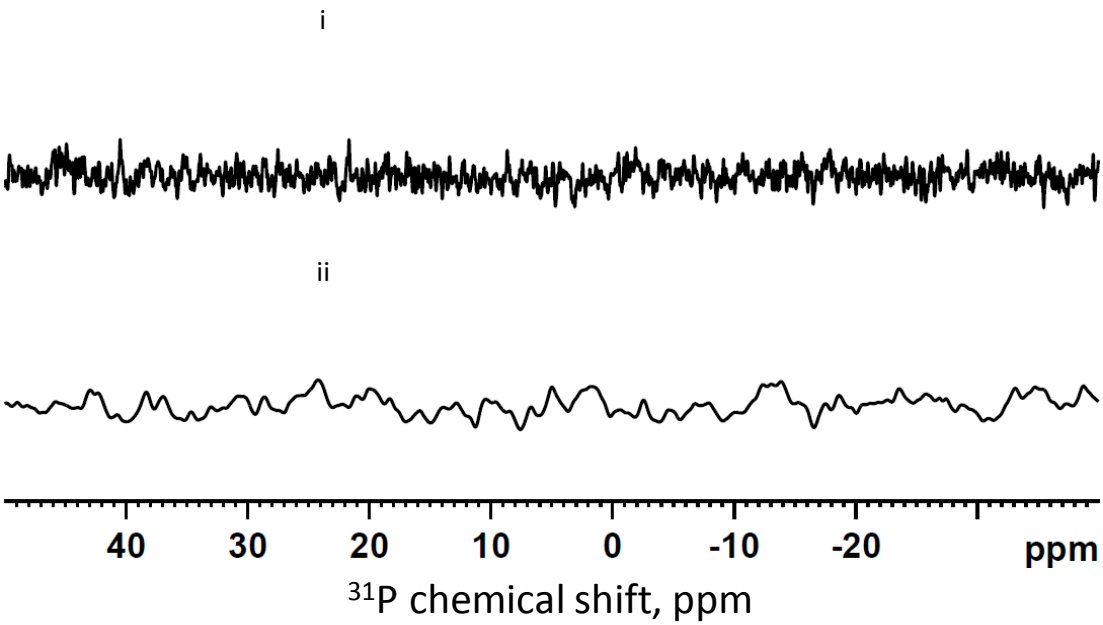

Figure 14. ^{31}P MAS-NMR spectra of the CPP-ACPF (i) and BGAF (ii) varnishes following the immersion.

Figure

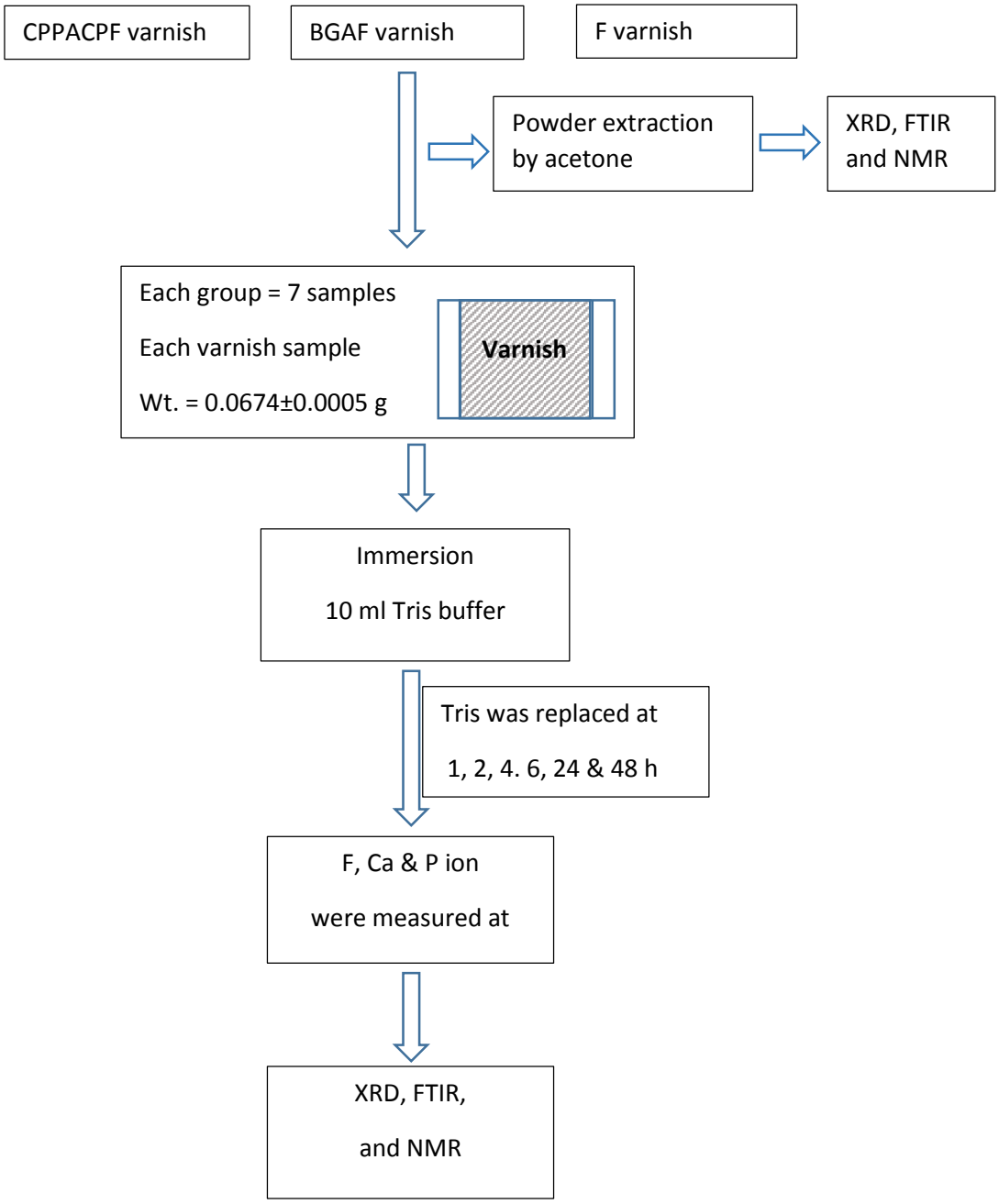

Figure 1. Study flow chart.

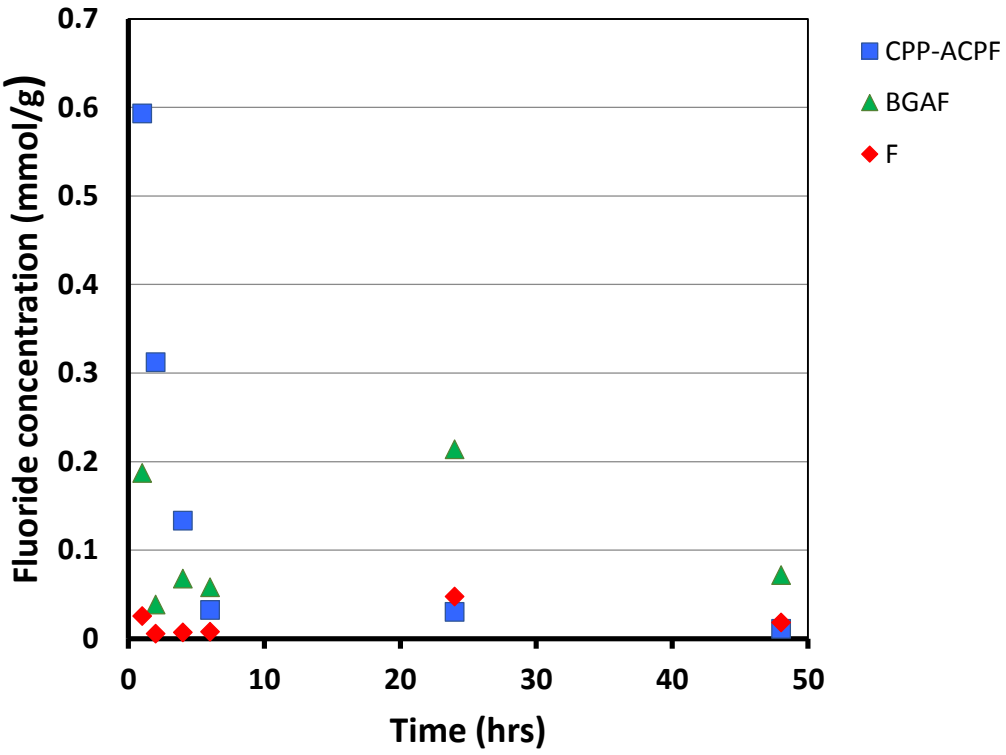

Figure 2. Non-cumulative F ion release at each time point in Tris buffer (mmol/g).

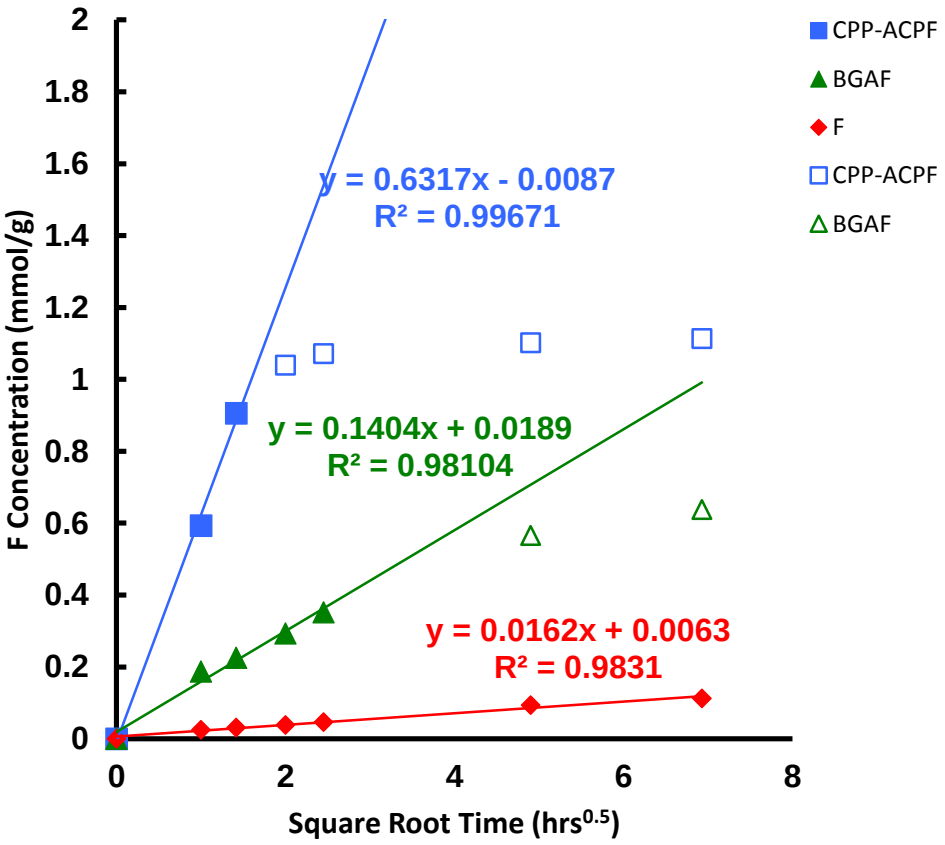

Figure 3. Cumulative F ion release of each varnish in the Tris buffer (mmol/g) using square root time on x – axis dependence at early times (lines). The empty shapes represent the actual values of fluoride ion release.

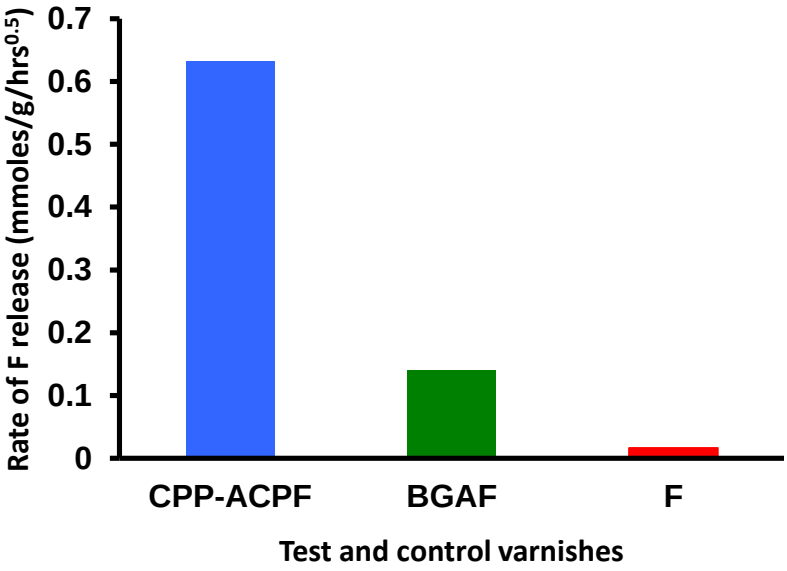

Figure 4. Rate of fluoride ion release of each varnish in the Tris buffer for the linear portion of release rate from Figure 3.

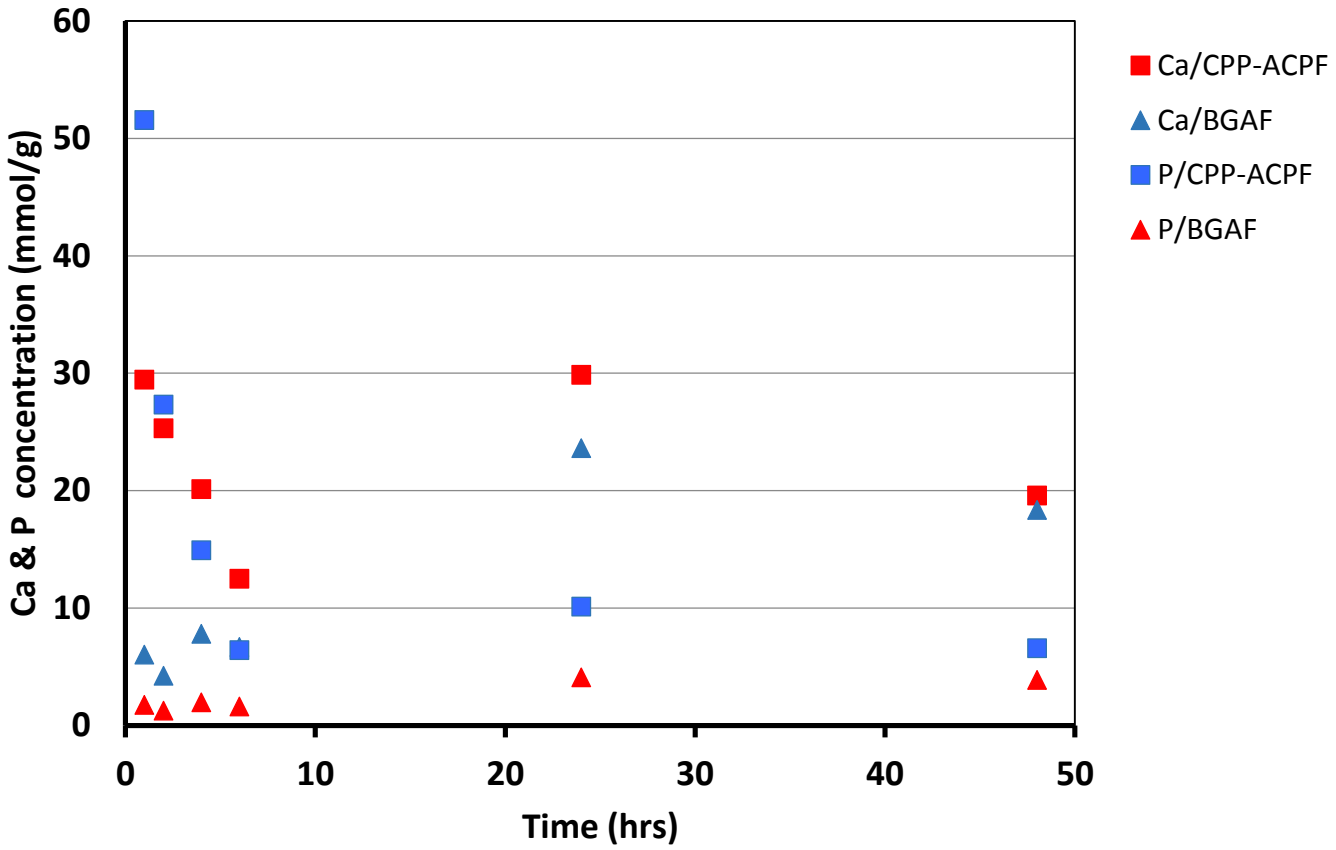

Figure 5. Non-cumulative calcium (Ca) and phosphorus (P) ion release for the CPP-ACPF, and BGAF varnishes in Tris buffer (mmol/g).

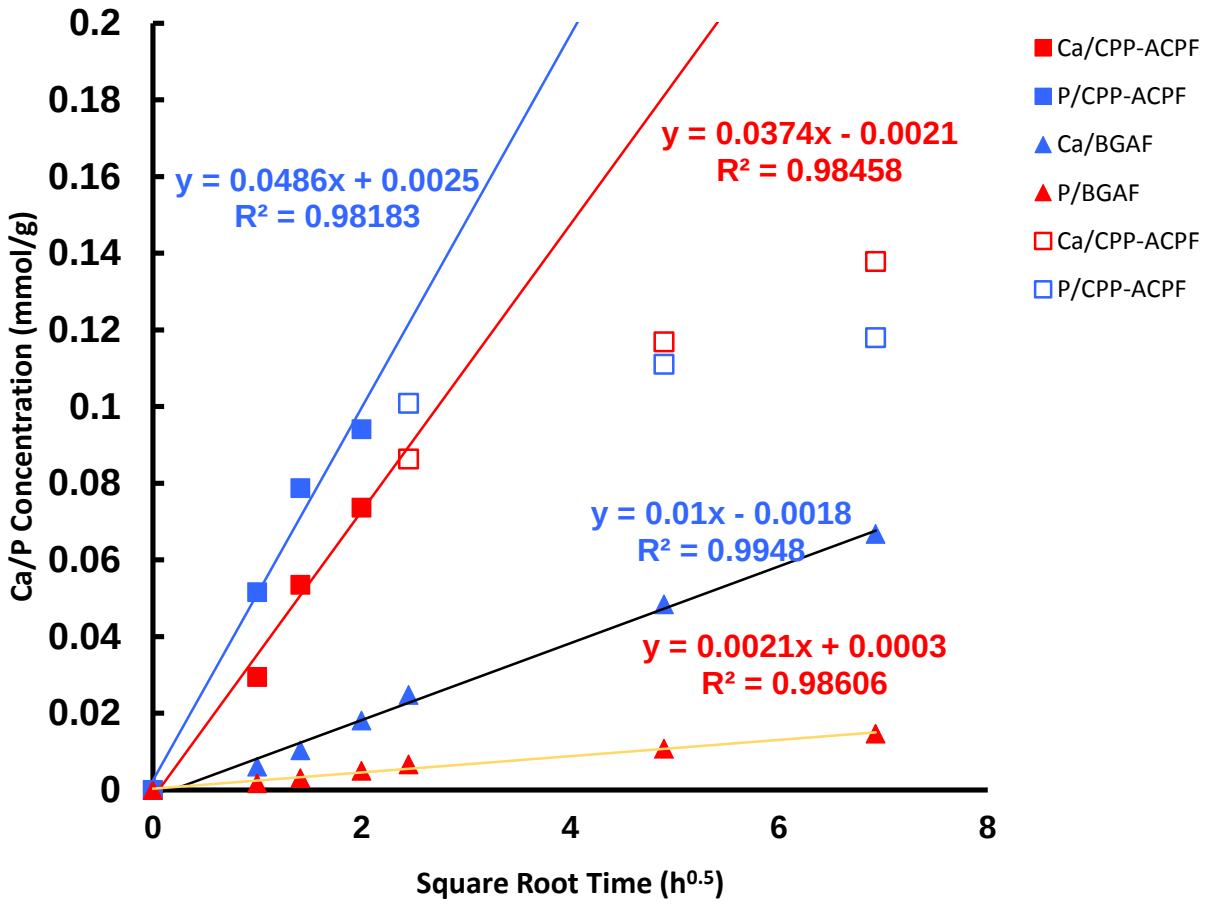

Figure 6. Cumulative calcium (Ca) and phosphorus (P) ion release over 48 h for the CPP-ACPF, and BGAF varnishes in Tris buffer (mmol/g) using square root time on x –axis. The empty shapes represent the actual values of ion release.

Square Root Time ($h^{-½}$)

Figure 7. Difference between the theoretical and measured Ca:P ratio for both the CPP-ACPF and BGAF.

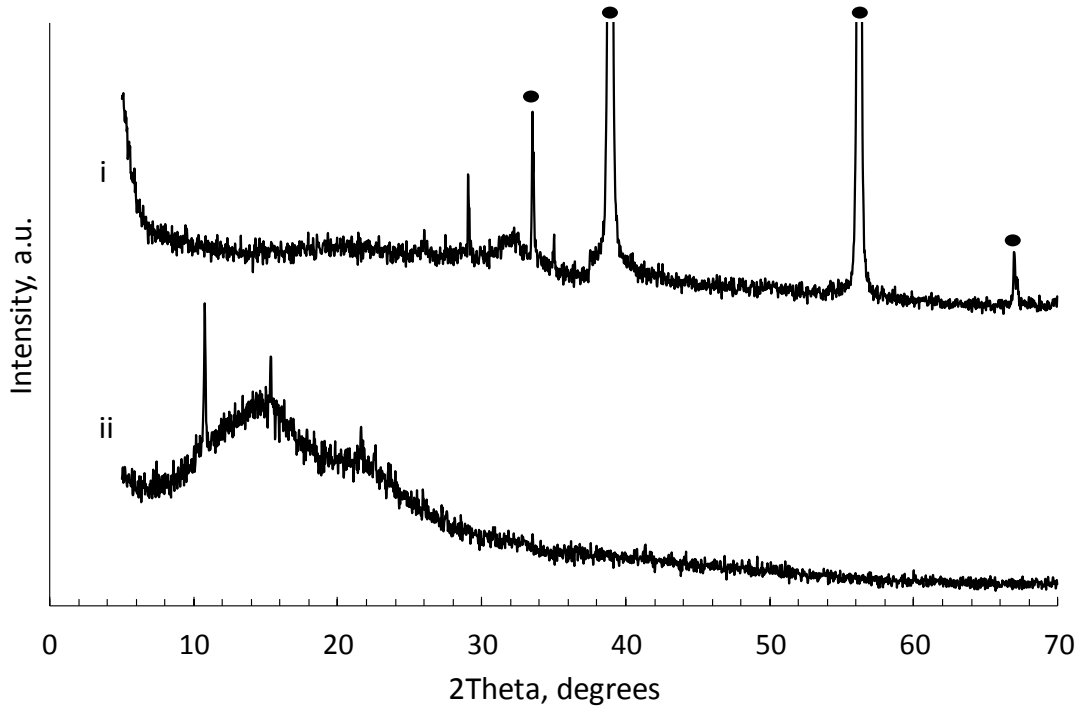

Figure 8. XRD pattern of CPP-ACPF varnish before (i) and after 48 h immersion in Tris buffer (ii). Filled circle indicates crystalline sodium fluoride.

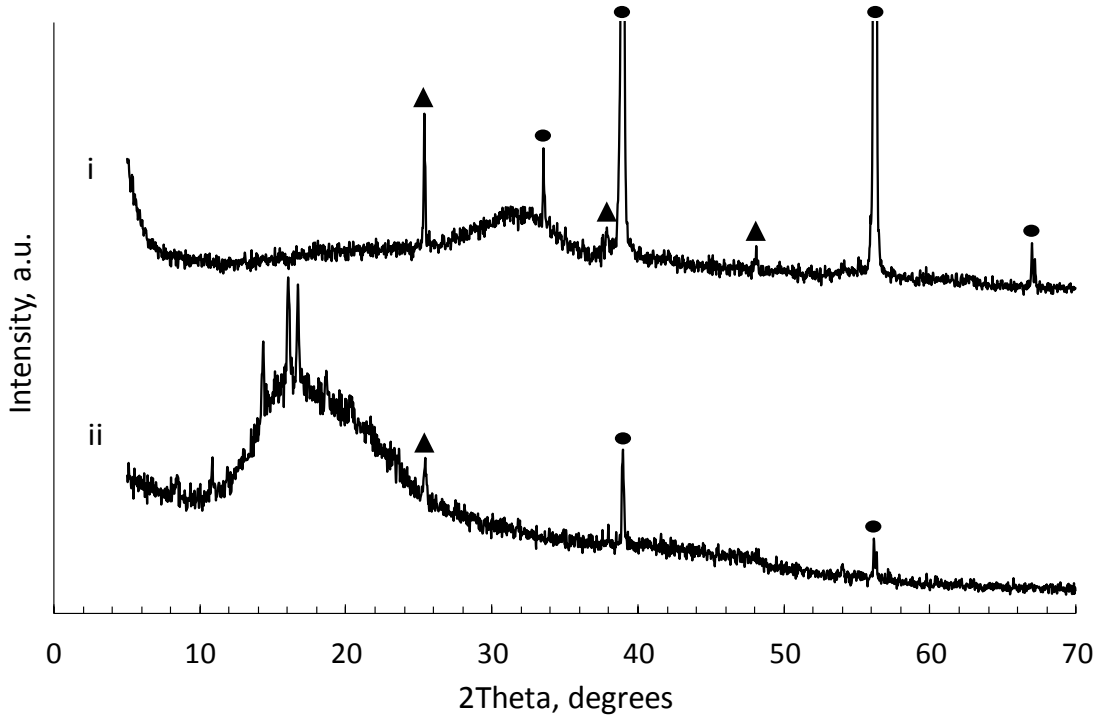

Figure 9. XRD pattern of BGAF varnish before (i) and after 48 hrs Tris immersion (ii). Filled circle indicates crystalline sodium fluoride and filled triangle is crystalline TiO_2.

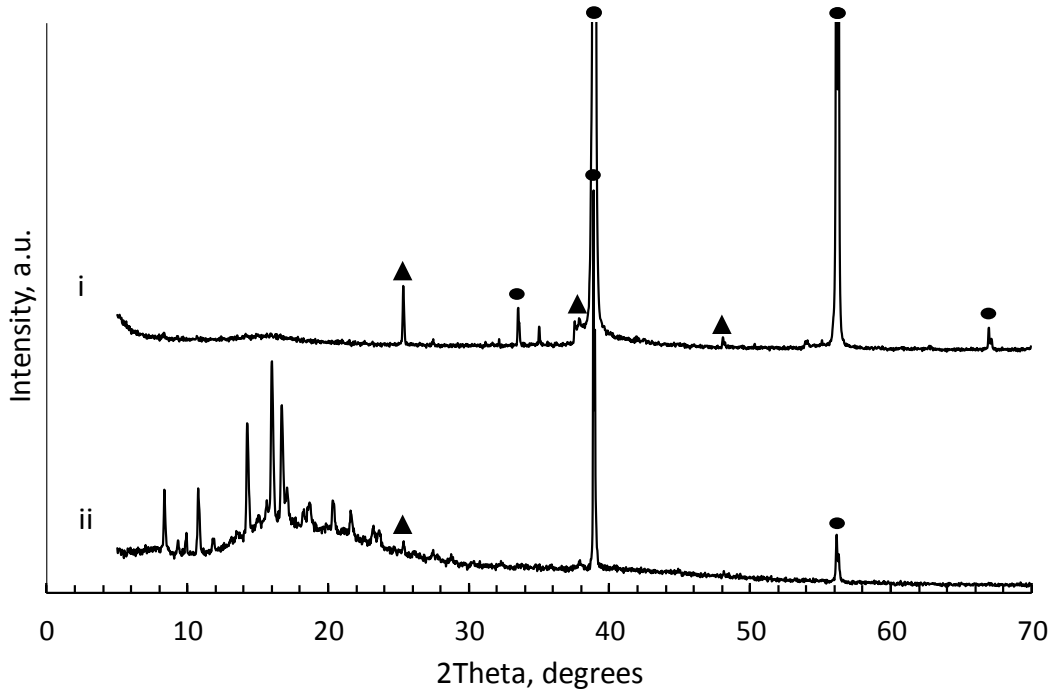

Figure 10. XRD pattern of F alone varnish before (i) and after 48 hrs Tris immersion (ii). Filled circle indicates crystalline sodium fluoride and filled triangle is crystalline TiO_2.

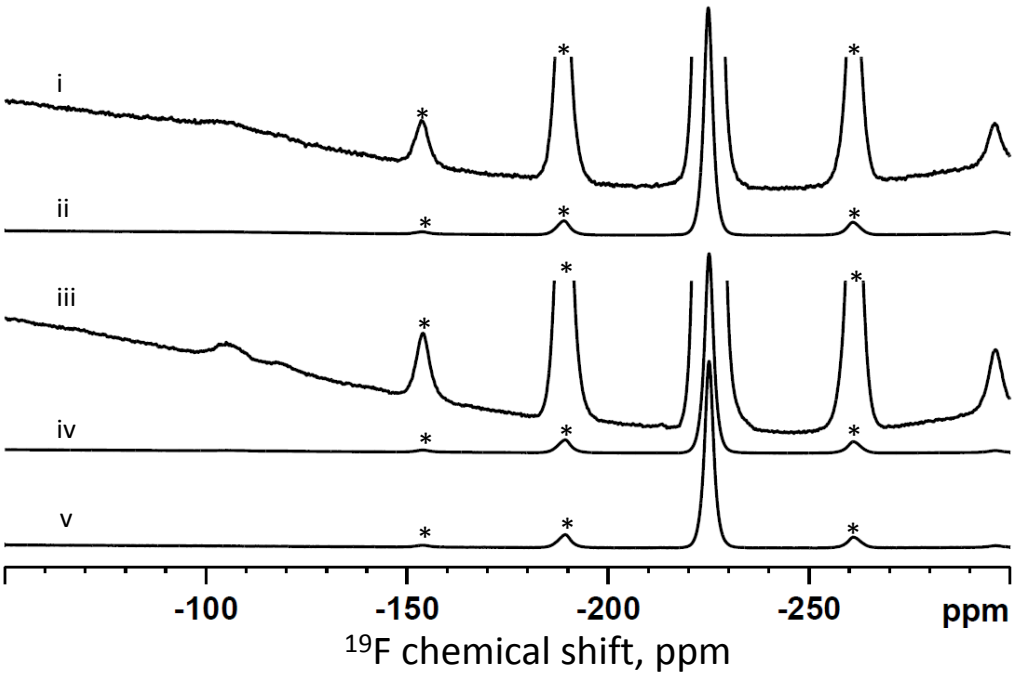
i
ii
iii
iv
v
-100
-150
-200
-250
ppm
19F chemical shift, ppm

Figure 11. ^{19}F MAS-NMR spectra of the test varnishes (powders extracted by acetone) before immersion; I and ii – CPP-ACPF, iii and iv – BGAF, v – F, where two spectra are shown the second spectrum is on an expanded scale. Asterisks show spinning side bands.

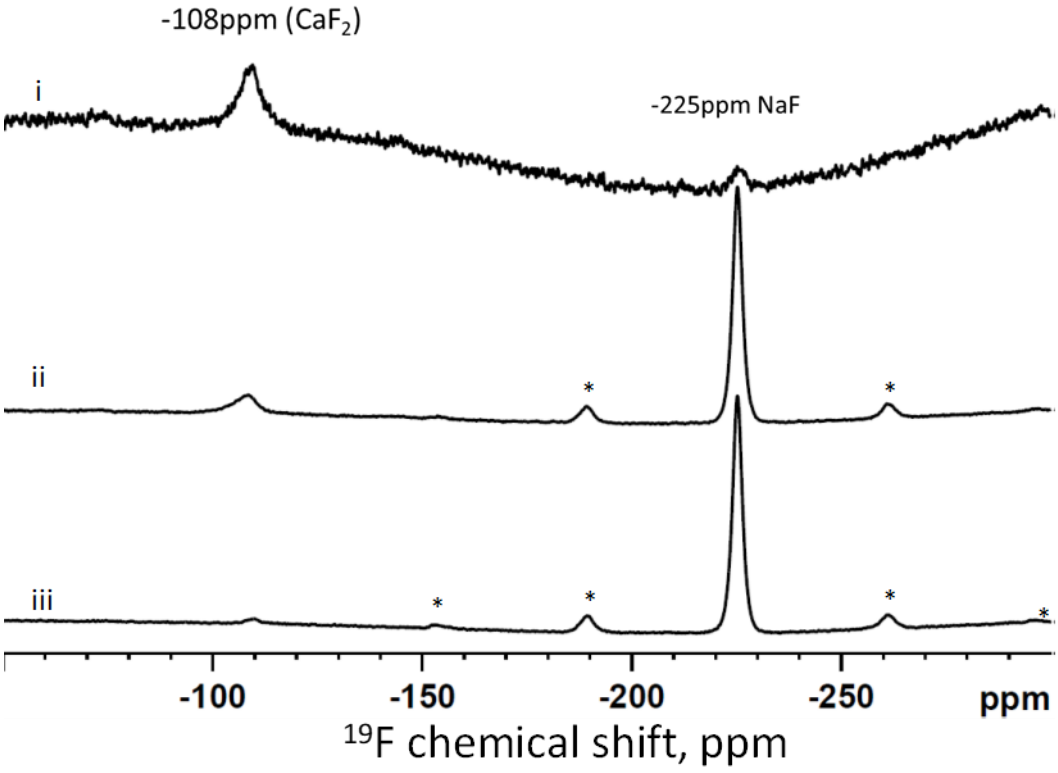

Figure 12. ^{19}F MAS-NMR spectra of the test varnishes following 48 hrs immersion in Tris buffer: i - CPP-ACPF; ii – BGAF; iii – F. Asterisks show spinning side bands.

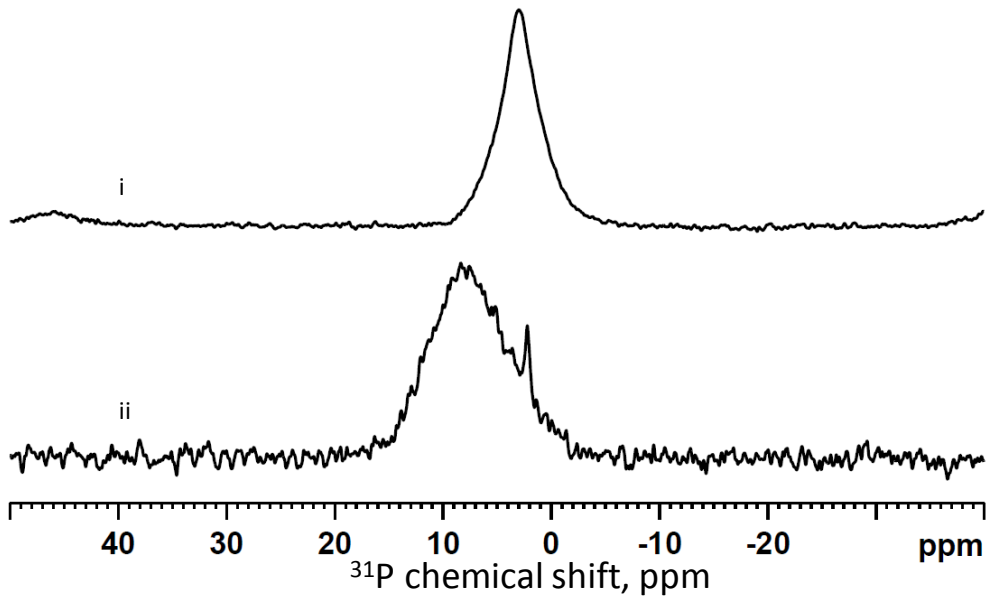

Figure 13. ^{31}P MAS-NMR spectrum of the CPP-ACPF (i) and BGAF (ii) varnishes (powders extracted by acetone) before immersion.

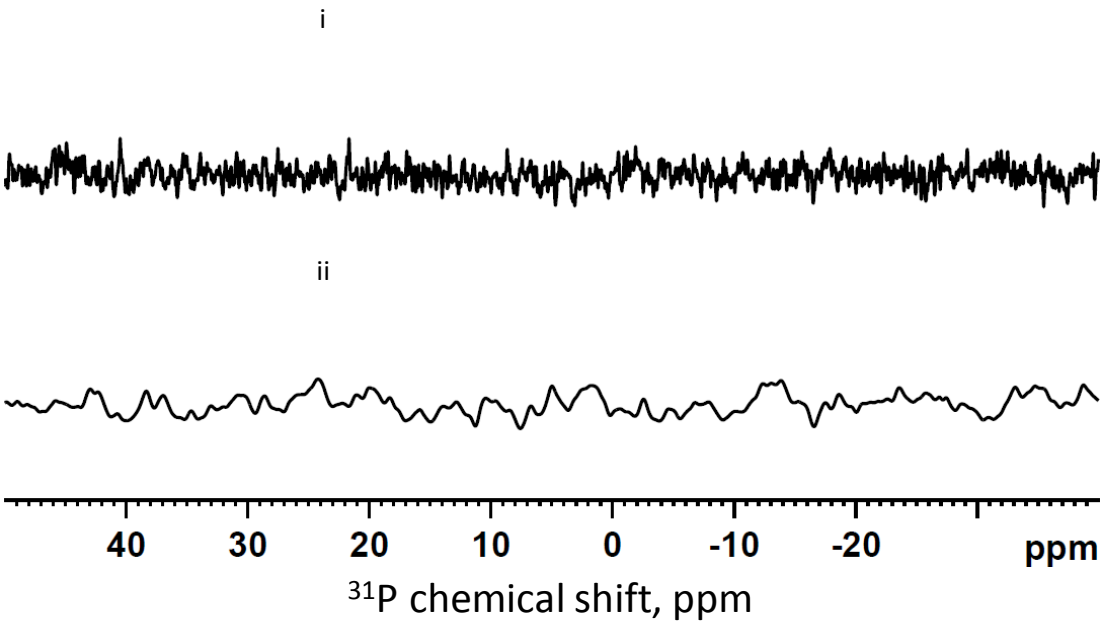

Figure 14. ^{31}P MAS-NMR spectra of the CPP-ACPF (i) and BGAF (ii) varnishes following 48 h immersion.

Table